New Results on the Structure of Baryons and their Excitations from Lattice QCD

Derek Leinweber
In collaboration with: Jonathan Hall, Waseem Kamleh, Adrian Kiratidis, Zhan-Wei Liu, Ben Menadue, Ben Owen, Tony Thomas, Jia-Jun Wu, Ross Young

SPECIAL RESEARCH CENTRE FOR THE SUBATOMIC STRUCTURE OF MATTER

THE UNIVERSITY of ADELAIDE

Outline

Lattice QCD Baryon Spectra at light quark masses

$\Lambda(1405)$, $N^*(1535)$, $N^*(1650)$ and $N'(1440)$ Resonances

Wave Functions of Nucleon Excitations

Isolation of the $\Lambda(1405)$ in Lattice QCD

Evidence the $\Lambda(1405)$ is a $\overline{K}N$ molecule

Hamiltonian Effective Field Theory Description of Spectra

The nature of the low-lying N Spectrum

Conclusions

Closely Related INPC Talks

- Adrian Kiratidis on Five-Quark Operators: Tuesday, R6, 2:40

Closely Related INPC Talks

- Adrian Kiratidis on Five-Quark Operators: Tuesday, R6, 2:40
- Ryan Bignell on Nucleon Polarizabilities: Friday, C1, 11:10

Closely Related INPC Talks

- Adrian Kiratidis on Five-Quark Operators: Tuesday, R6, 2:40
- Ryan Bignell on Nucleon Polarizabilities: Friday, C1, 11:10
- Zhan-Wei Liu on Hamiltonian Effective Field Theory: Friday, C1, 11:25

Closely Related INPC Talks

- Adrian Kiratidis on Five-Quark Operators: Tuesday, R6, 2:40
- Ryan Bignell on Nucleon Polarizabilities: Friday, C1, 11:10
- Zhan-Wei Liu on Hamiltonian Effective Field Theory: Friday, C1, 11:25
- Jonathan Hall on the magnetic moment of the $\Lambda(1405)$, Friday, C1, 12:10

Closely Related INPC Talks

- Adrian Kiratidis on Five-Quark Operators: Tuesday, R6, 2:40
- Ryan Bignell on Nucleon Polarizabilities: Friday, C1, 11:10
- Zhan-Wei Liu on Hamiltonian Effective Field Theory: Friday, C1, 11:25
- Jonathan Hall on the magnetic moment of the $\Lambda(1405)$, Friday, C1, 12:10
- Finn Stokes on Excited State Form Factors: Immediately following this talk.

CSSM Simulation Details

Based on the PACS-CS $(2+1)$-flavour ensembles, available through the ILDG.

S. Aoki *et al* (PACS-CS Collaboration), Phys. Rev. D **79**, 034503 (2009)

CSSM Simulation Details

Based on the PACS-CS $(2+1)$-flavour ensembles, available through the ILDG.

S. Aoki *et al* (PACS-CS Collaboration), Phys. Rev. D **79**, 034503 (2009)

- Lattice size of $32^3 \times 64$ with $\beta = 1.90$. $L \simeq 3$ fm.

CSSM Simulation Details

Based on the PACS-CS $(2+1)$-flavour ensembles, available through the ILDG.

S. Aoki *et al* (PACS-CS Collaboration), Phys. Rev. D **79**, 034503 (2009)

- Lattice size of $32^3 \times 64$ with $\beta = 1.90$. $L \simeq 3$ fm.
- 5 pion masses, ranging from 640 MeV down to 156 MeV.

CSSM Simulation Details

Based on the PACS-CS $(2+1)$-flavour ensembles, available through the ILDG.

S. Aoki *et al* (PACS-CS Collaboration), Phys. Rev. D **79**, 034503 (2009)

- Lattice size of $32^3 \times 64$ with $\beta = 1.90$. $L \simeq 3$ fm.
- 5 pion masses, ranging from 640 MeV down to 156 MeV.
- The strange quark κ_s is held fixed as the light quark masses vary.
  - Changes in the strange quark contributions are environmental effects.

Positive Parity Nucleon Spectrum: CSSM

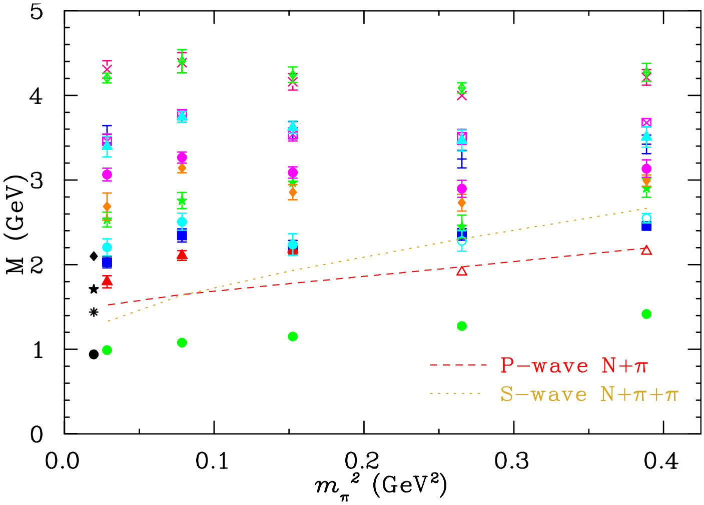

Comparison: Hadron Spectrum Collaboration (HSC)

- “Excited state baryon spectroscopy from lattice QCD,”
  R. G. Edwards, J. J. Dudek, D. G. Richards and S. J. Wallace,
  Phys. Rev. D **84** (2011) 074508 arXiv:1104.5152 [hep-ph].

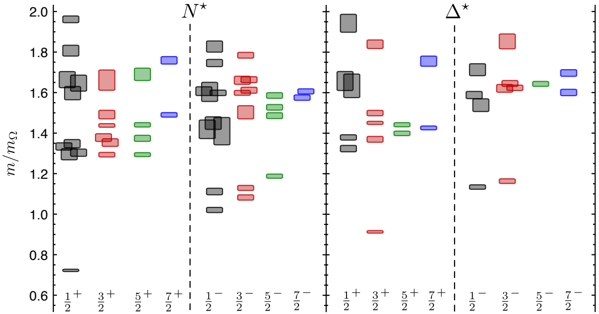

CSSM & HSC Comparison: Positive Parity CSSM

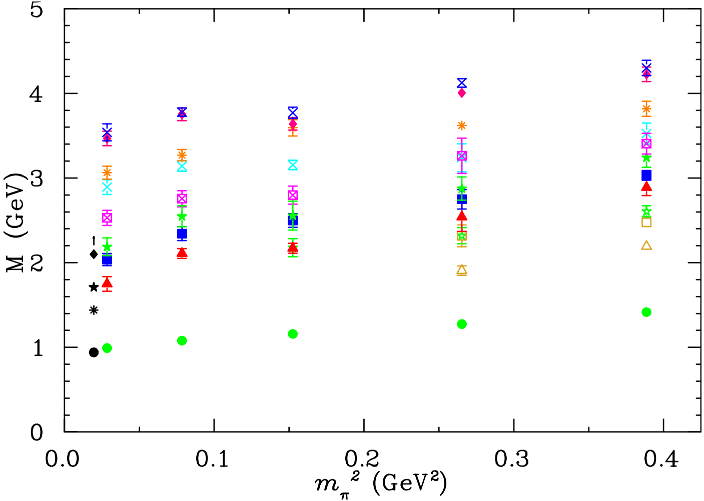

CSSM & HSC Comparison: Positive Parity

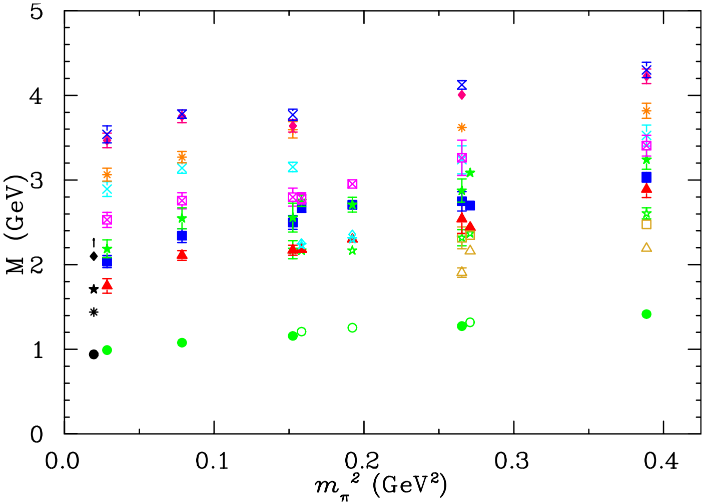

CSSM & HSC Comparison: Negative Parity CSSM

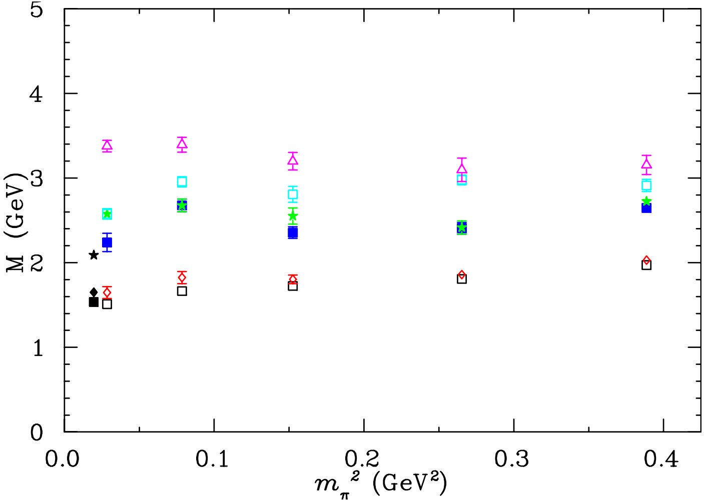

CSSM & HSC Comparison: Negative Parity

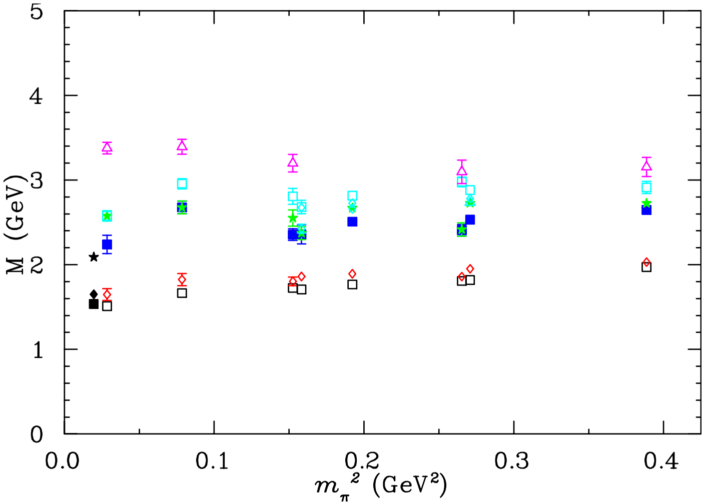

Further Information

- "Roper Resonance in 2+1 Flavor QCD,"
  M. S. Mahbub, *et al.* [CSSM],
  Phys. Lett. B **707** (2012) 389
  arXiv:1011.5724 [hep-lat],

- "Low-lying Odd-parity States of the Nucleon in Lattice QCD,"
  M. Selim Mahbub, *et al.* [CSSM],
  Phys. Rev. D Rapid Comm. **87** (2013) 011501,
  arXiv:1209.0240 [hep-lat]

- "Structure and Flow of the Nucleon Eigenstates in Lattice QCD,"
  M. S. Mahbub, *et al.* [CSSM],
  Phys. Rev. D **87** (2013) 9, 094506
  arXiv:1302.2987 [hep-lat].

Wave Functions of Positive-Parity Nucleons

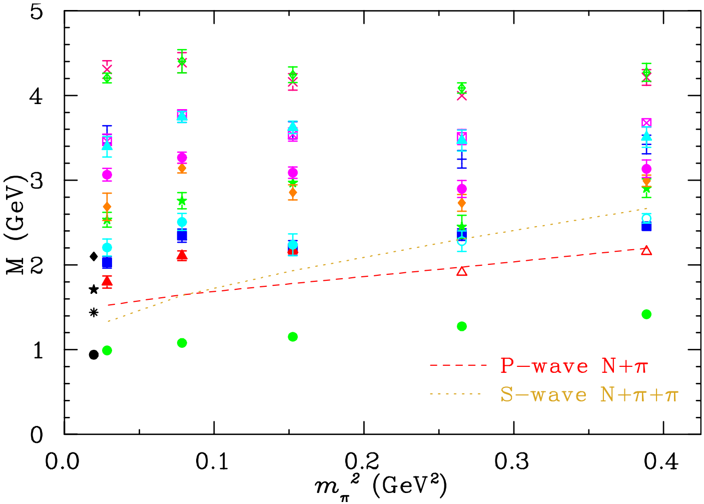

d-quark probability density in ground state proton (CSSM)

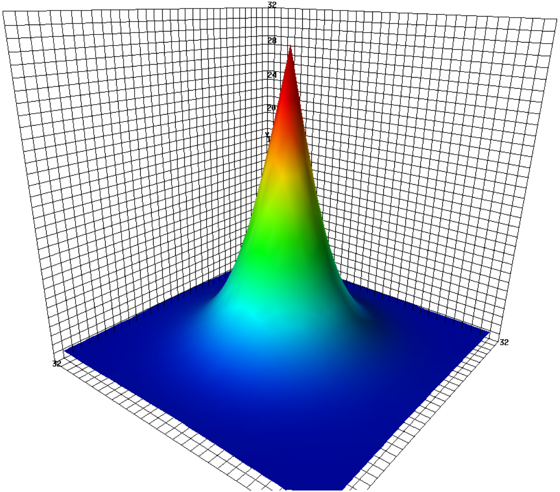

d-quark probability density in 1st excited state of proton (CSSM)

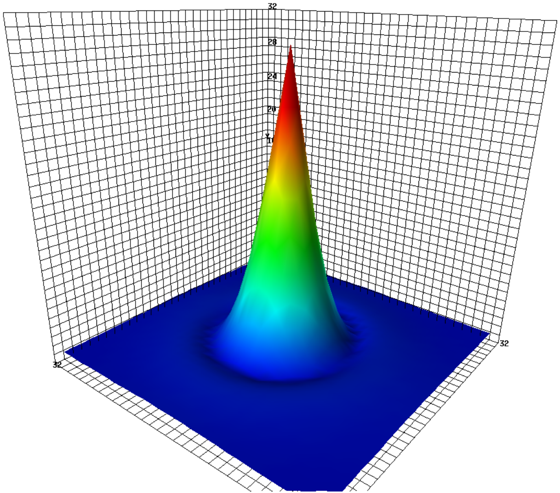

d-quark probability density in $N = 3$ excited state of proton (CSSM)

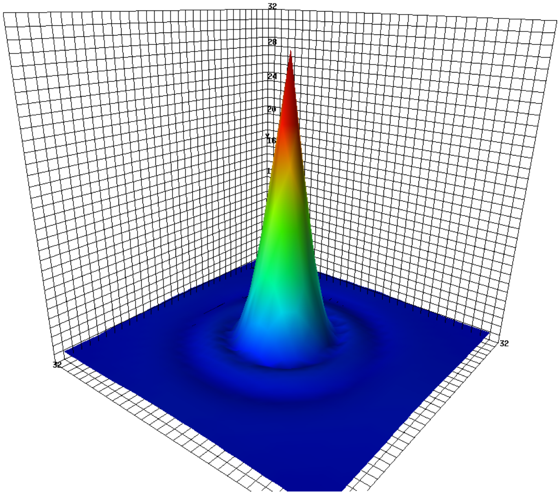

Comparison with the Simple Quark Model - CSSM

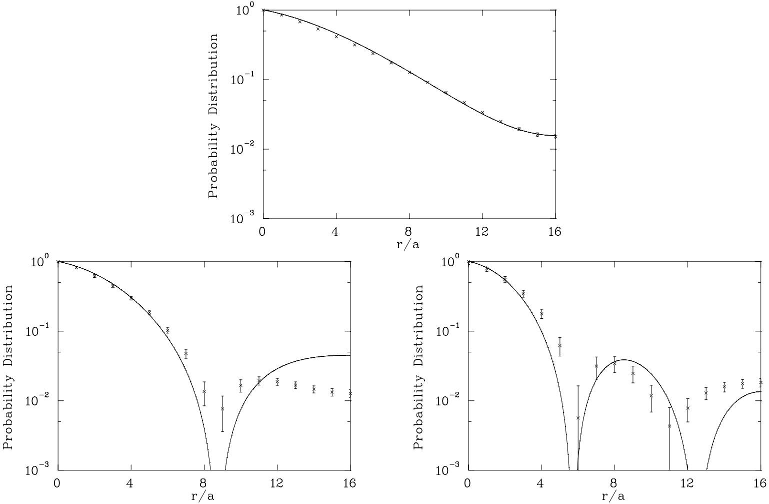

Finite-Volume Effects in Wave Functions

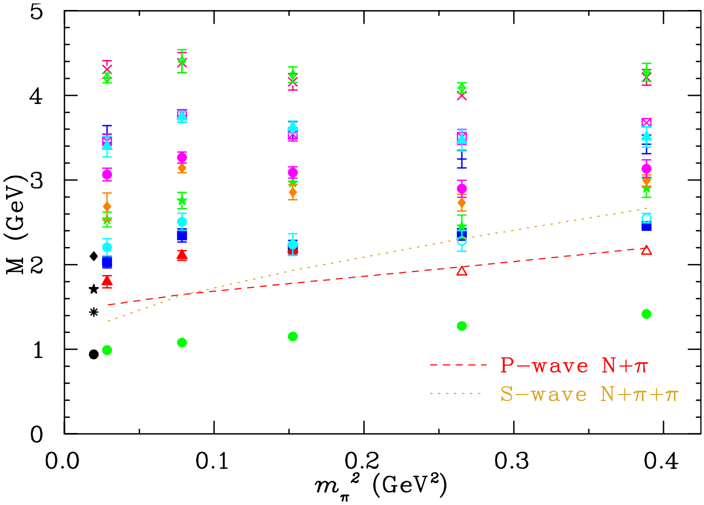

Finite-Volume Effect in $N = 2$ excited state: $m_\pi = 702$ MeV

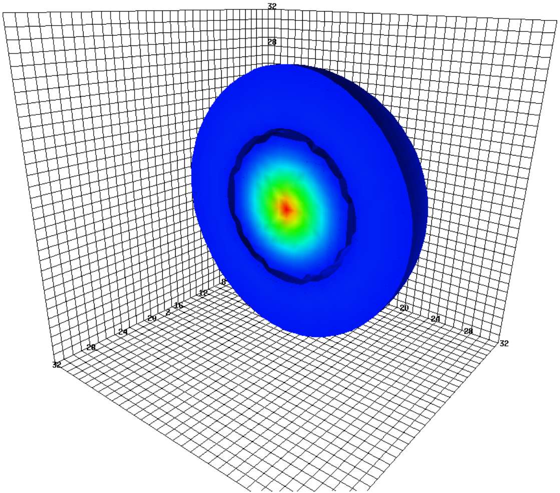

Finite-Volume Effect in $N = 2$ excited state: $m_\pi = 570$ MeV

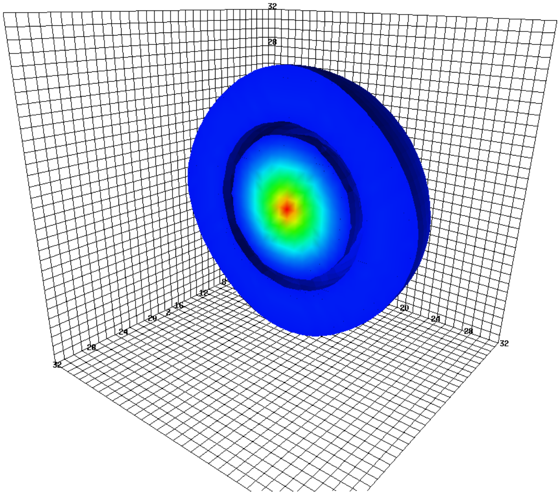

Finite-Volume Effect in $N = 2$ excited state: $m_\pi = 411$ MeV

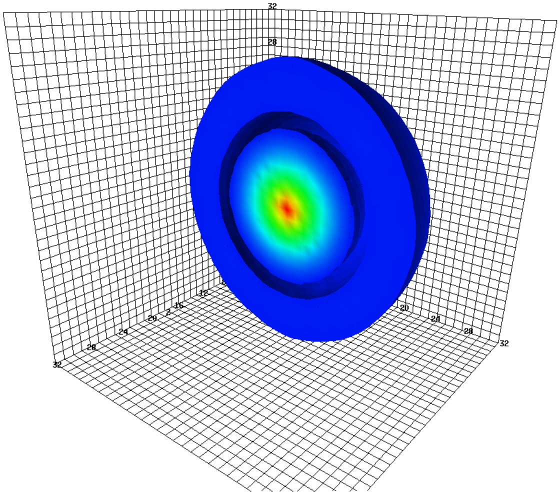

Finite-Volume Effect in $N = 2$ excited state: $m_\pi = 296$ MeV

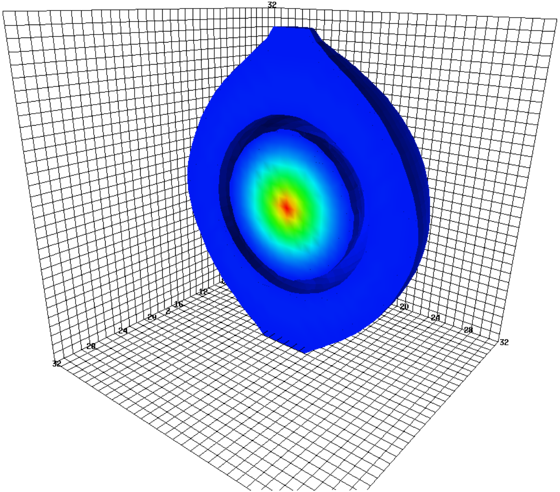

Finite-Volume Effect in $N = 2$ excited state: $m_\pi = 156$ MeV

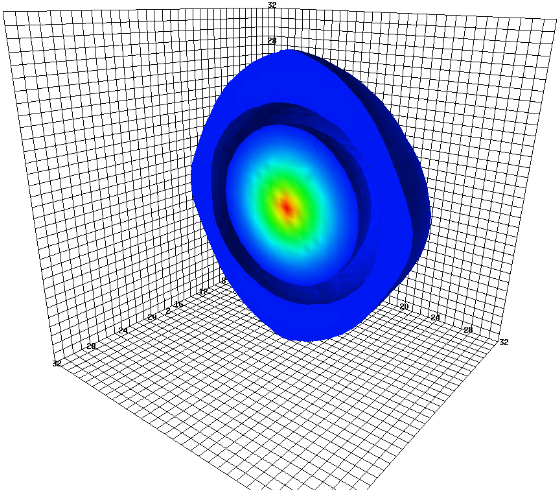

d-quark probability density in 1st excited state of proton (CSSM)

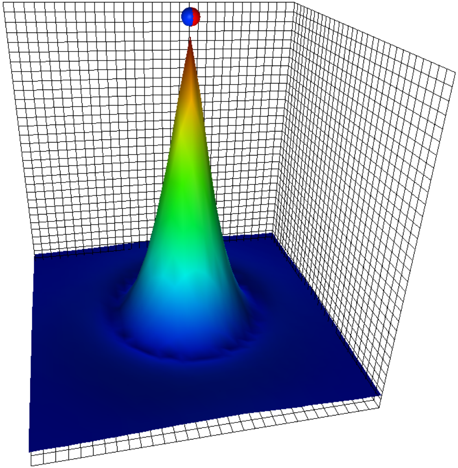

d-quark probability density in 1st excited state of proton (CSSM)

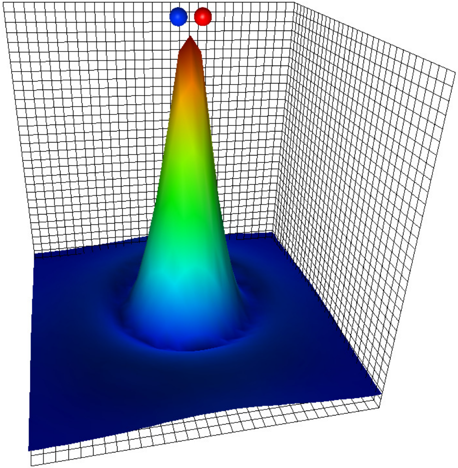

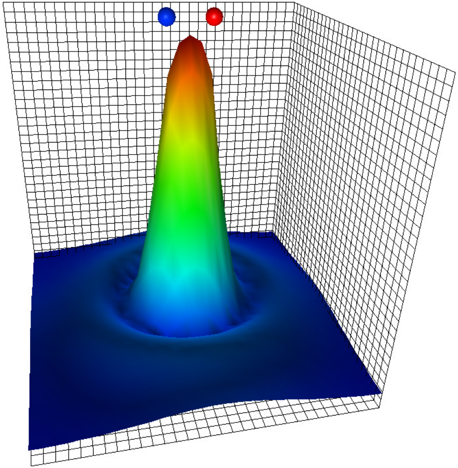

d-quark probability density in 1st excited state of proton (CSSM)

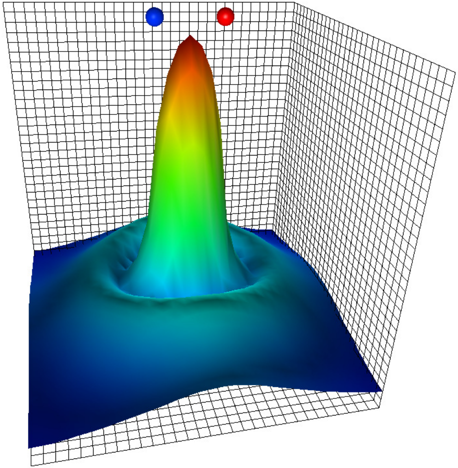

d-quark probability density in 1st excited state of proton (CSSM)

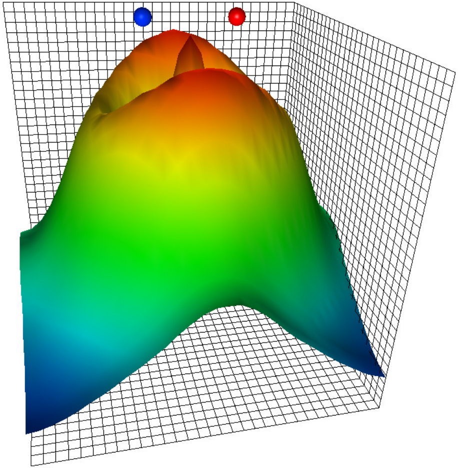

d-quark probability density in 1st excited state of proton (CSSM)

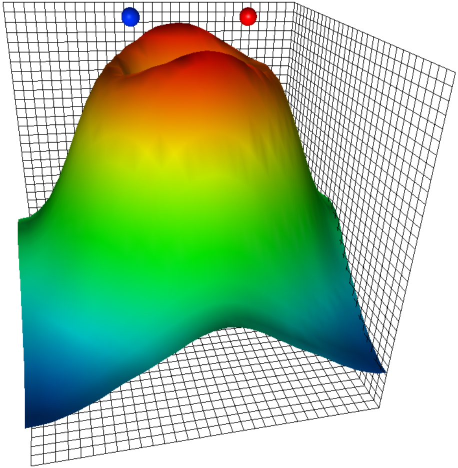

d-quark probability density in 1st excited state of proton (CSSM)

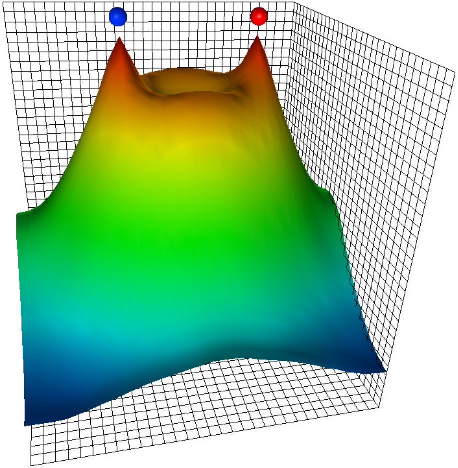

d-quark probability density in 1st excited state of proton (CSSM)

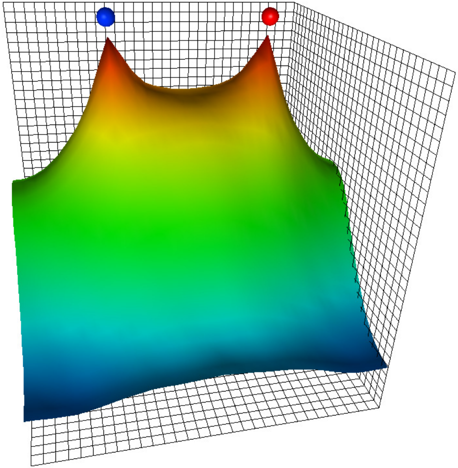

d-quark probability density in 4th excited state of proton (CSSM)

PHYSICAL REVIEW D

particles, fields, gravitation, and cosmology

Highlights Recent Accepted Authors Referees Search About

Kaleidoscope

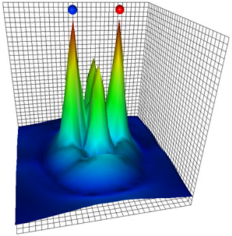

From the article:

Nucleon excited state wave functions from lattice QCD

Dale S. Roberts, Waseem Kamleh, and Derek B. Leinweber

Phys. Rev. D **89**, 074501 (2014)

The $\Lambda(1405)$ and Lattice QCD

Our 2012 work successfully isolated three low-lying odd-parity spin-1/2 states.

B. Menadue, W. Kamleh, D. B. Leinweber, M. S. Mahbub, Phys. Rev. Lett. **108**, 112001 (2012)

- An extrapolation of the trend of the lowest state reproduces the mass of the $\Lambda(1405)$.
- Subsequent studies have confirmed these results.

G. P. Engel, C. B. Lang, A. Schäfer, Phys. Rev. D **87**, 034502 (2013)

$\Lambda(1405)$ and Baryon Octet dominated states

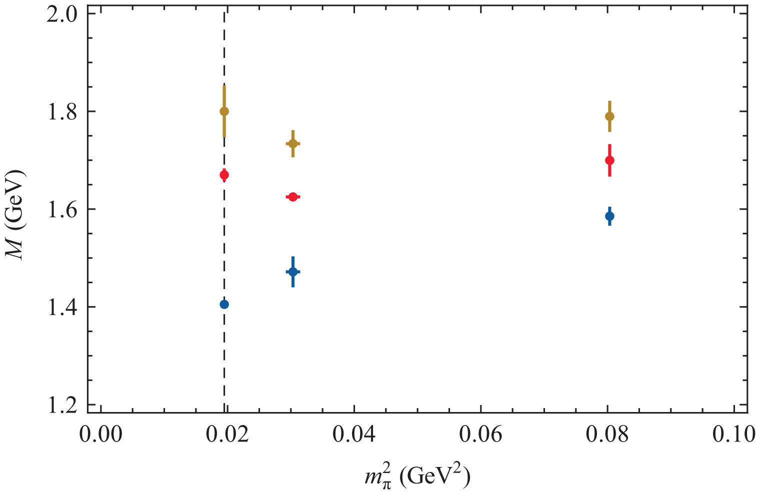

Operators Used in $\Lambda(1405)$ Analysis

We consider local three-quark operators with the correct quantum numbers for the Λ channel, including

- Flavour-octet operators

$$\chi_1^8 = \frac{1}{\sqrt{6}} \varepsilon^{abc} \left(2(u^a C\gamma_5 d^b)s^c + (u^a C\gamma_5 s^b)d^c - (d^a C\gamma_5 s^b)u^c \right)$$
$$\chi_2^8 = \frac{1}{\sqrt{6}} \varepsilon^{abc} \left(2(u^a C d^b)\gamma_5 s^c + (u^a C s^b)\gamma_5 d^c - (d^a C s^b)\gamma_5 u^c \right)$$

- Flavour-singlet operator

$$\chi^1 = 2\varepsilon^{abc} \left((u^a C\gamma_5 d^b)s^c - (u^a C\gamma_5 s^b)d^c + (d^a C\gamma_5 s^b)u^c \right)$$

- Consideration of 16 and 100 sweeps of gauge-invariant Gaussian smearing provides a 6×6 correlation matrix.

Flavour structure of the $\Lambda(1405)$

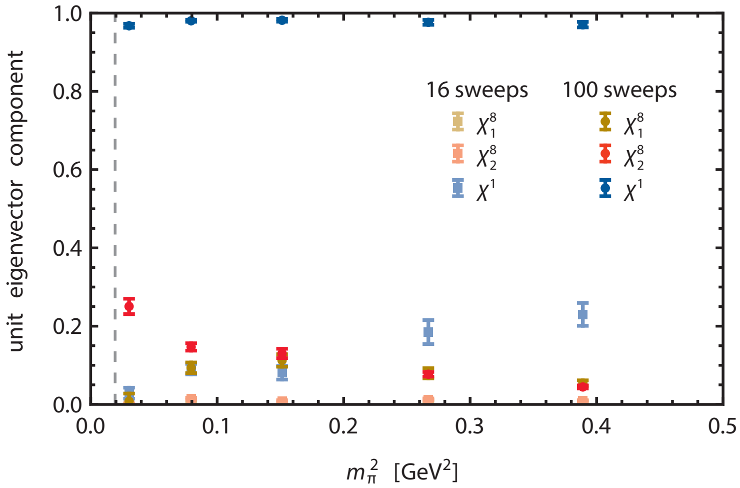

The importance of eigenstate isolation (red)

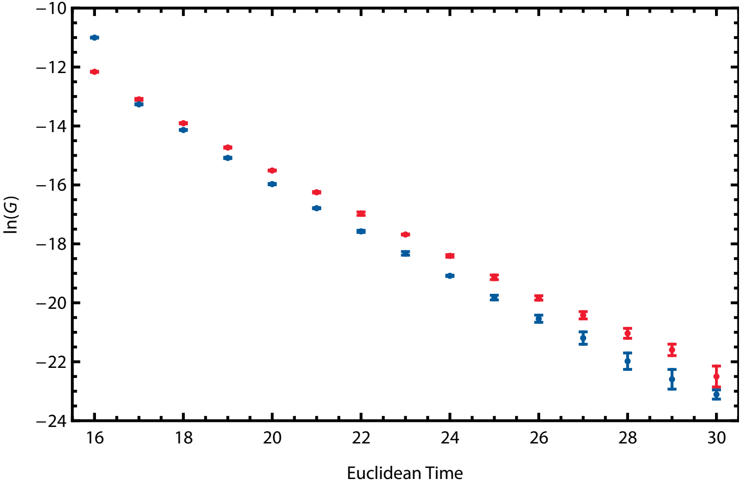

Probing with the electromagnetic current

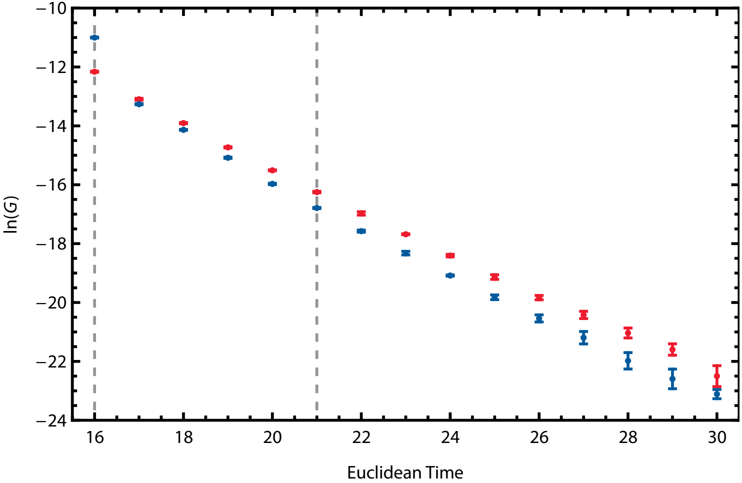

Only the projected correlator has acceptable χ^2/dof

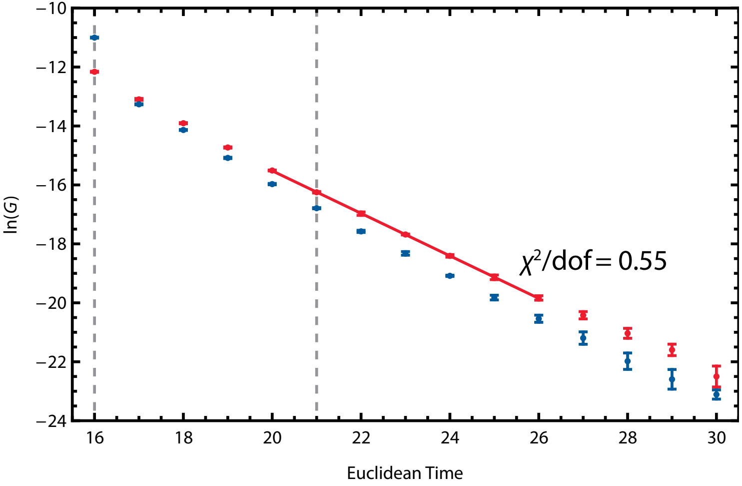

Is the $\Lambda(1405)$ really exotic?

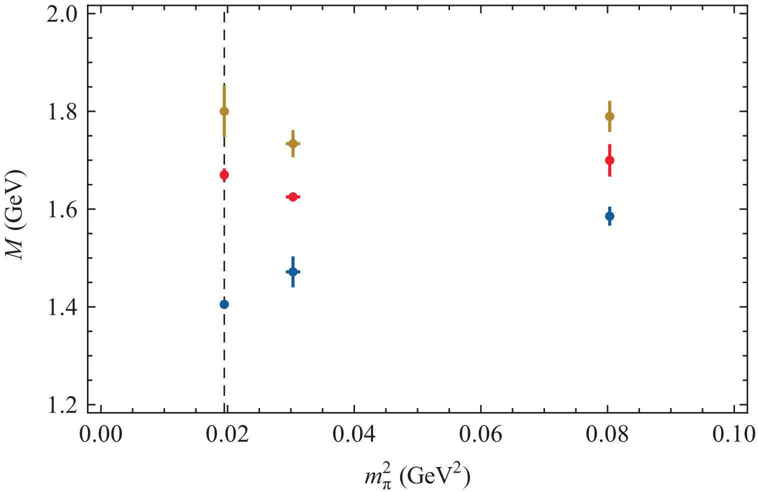

Strange Magnetic Form Factor of the $\Lambda(1405)$

- Provides direct insight into the possible dominance of a molecular $\overline{K}N$ bound state.

Strange Magnetic Form Factor of the $\Lambda(1405)$

- Provides direct insight into the possible dominance of a molecular $\overline{K}N$ bound state.
- In forming such a molecular state, the $\Lambda(u, d, s)$ valence quark configuration is complemented by
  - A $u, \overline{u}$ pair making a $K^-(s, \overline{u})$ - proton (u, u, d) bound state, or
  - A $d, \overline{d}$ pair making a $\overline{K}^0(s, \overline{d})$ - neutron (d, d, u) bound state.

Strange Magnetic Form Factor of the $\Lambda(1405)$

- Provides direct insight into the possible dominance of a molecular $\overline{K}N$ bound state.
- In forming such a molecular state, the $\Lambda(u, d, s)$ valence quark configuration is complemented by
  - A $u, \overline{u}$ pair making a $K^-(s, \overline{u})$ - proton (u, u, d) bound state, or
  - A $d, \overline{d}$ pair making a $\overline{K}^0(s, \overline{d})$ - neutron (d, d, u) bound state.
- In both cases the strange quark is confined within a spin-0 kaon and has no preferred spin orientation.

Strange Magnetic Form Factor of the $\Lambda(1405)$

- Provides direct insight into the possible dominance of a molecular $\overline{K}N$ bound state.
- In forming such a molecular state, the $\Lambda(u, d, s)$ valence quark configuration is complemented by
  - A $u, \overline{u}$ pair making a $K^-(s, \overline{u})$ - proton (u, u, d) bound state, or
  - A $d, \overline{d}$ pair making a $\overline{K}^0(s, \overline{d})$ - neutron (d, d, u) bound state.
- In both cases the strange quark is confined within a spin-0 kaon and has no preferred spin orientation.
- To conserve parity, the kaon has zero orbital angular momentum.

Strange Magnetic Form Factor of the $\Lambda(1405)$

- Provides direct insight into the possible dominance of a molecular $\overline{K}N$ bound state.
- In forming such a molecular state, the $\Lambda(u, d, s)$ valence quark configuration is complemented by
  - A $u, \overline{u}$ pair making a $K^-(s, \overline{u})$ - proton (u, u, d) bound state, or
  - A $d, \overline{d}$ pair making a $\overline{K}^0(s, \overline{d})$ - neutron (d, d, u) bound state.
- In both cases the strange quark is confined within a spin-0 kaon and has no preferred spin orientation.
- To conserve parity, the kaon has zero orbital angular momentum.
- Thus, the strange quark does not contribute to the magnetic form factor of the $\Lambda(1405)$ when it is dominated by a $\overline{K}N$ molecule.

$\mathcal{G}_M$ for the $\Lambda(1405)$ at $Q^2 \sim 0.16\,\mathrm{GeV}^2$

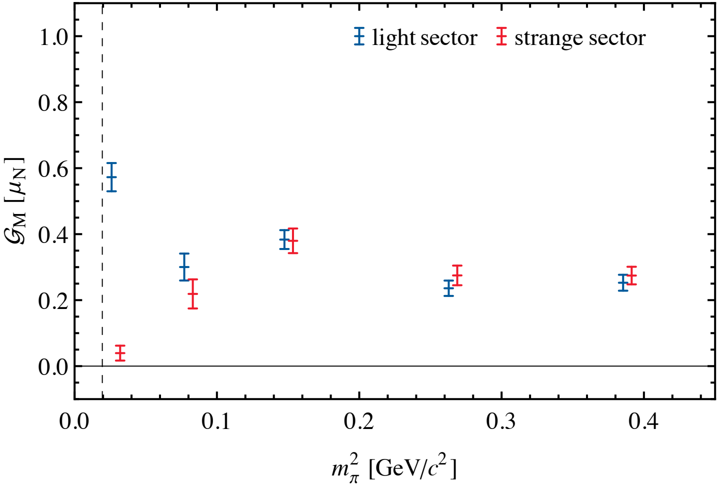

$\mathcal{G}_M$ for the $\Lambda(1405)$ at $Q^2 \sim 0.16\ \mathrm{GeV}^2$

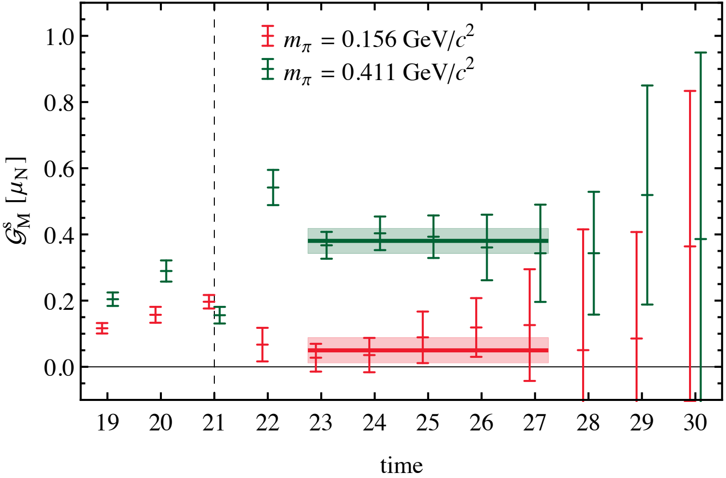

Hamiltonian Effective Field Theory

- J. M. M. Hall, *et al.* [CSSM]
  "Lattice QCD Evidence that the $\Lambda(1405)$ Resonance is an Antikaon Nucleon Molecule"
  Phys. Rev. Lett. **114**, 132002 (2015), arXiv:1411.3402 [hep-lat]

Hamiltonian Effective Field Theory

- J. M. M. Hall, *et al.* [CSSM]
  "Lattice QCD Evidence that the Λ(1405) Resonance is an Antikaon Nucleon Molecule"
  Phys. Rev. Lett. **114**, 132002 (2015), arXiv:1411.3402 [hep-lat]

- Z. W. Liu, J. M. M. Hall, DBL, A. W. Thomas and J. J. Wu.
  "Structure of the Λ(1405) from Hamiltonian effective field theory"
  arXiv:1607.05856 [nucl-th]

Hamiltonian Effective Field Theory

- J. M. M. Hall, *et al.* [CSSM]
  "Lattice QCD Evidence that the $\Lambda(1405)$ Resonance is an Antikaon Nucleon Molecule"
  Phys. Rev. Lett. **114**, 132002 (2015), arXiv:1411.3402 [hep-lat]

- Z. W. Liu, J. M. M. Hall, DBL, A. W. Thomas and J. J. Wu.
  "Structure of the $\Lambda(1405)$ from Hamiltonian effective field theory"
  arXiv:1607.05856 [nucl-th]

- Z. W. Liu, W. Kamleh, DBL, F. M. Stokes, A. W. Thomas and J. J. Wu,
  "Hamiltonian EFT study of the $N^*(1535)$ resonance in lattice QCD,"
  Phys. Rev. Lett. **116** (2016) 082004, [arXiv:1512.00140 [hep-lat]]

Hamiltonian Effective Field Theory

- J. M. M. Hall, *et al.* [CSSM]
  "Lattice QCD Evidence that the $\Lambda(1405)$ Resonance is an Antikaon Nucleon Molecule"
  Phys. Rev. Lett. **114**, 132002 (2015), arXiv:1411.3402 [hep-lat]

- Z. W. Liu, J. M. M. Hall, DBL, A. W. Thomas and J. J. Wu.
  "Structure of the $\Lambda(1405)$ from Hamiltonian effective field theory"
  arXiv:1607.05856 [nucl-th]

- Z. W. Liu, W. Kamleh, DBL, F. M. Stokes, A. W. Thomas and J. J. Wu,
  "Hamiltonian EFT study of the $N^*(1535)$ resonance in lattice QCD,"
  Phys. Rev. Lett. **116** (2016) 082004, [arXiv:1512.00140 [hep-lat]]

- Z. W. Liu, W. Kamleh, DBL, F. M. Stokes, A. W. Thomas and J. J. Wu,
  "Hamiltonian EFT study of the $N^*(1440)$ resonance in lattice QCD,"
  arXiv:1607.04536 [nucl-th]

Hamiltonian Effective Field Theory Model

- Consider the $\Lambda(1405)$.

Hamiltonian Effective Field Theory Model

- Consider the $\Lambda(1405)$.
- The four octet meson-baryon interaction channels of the $\Lambda(1405)$ are considered: $\pi\Sigma$, $\overline{K}N$, $K\Xi$ and $\eta\Lambda$.

Hamiltonian Effective Field Theory Model

- Consider the $\Lambda(1405)$.
- The four octet meson-baryon interaction channels of the $\Lambda(1405)$ are considered: $\pi\Sigma$, $\overline{K}N$, $K\Xi$ and $\eta\Lambda$.
- A single-particle state with bare mass, $m_0 + \alpha_0\, m_\pi^2$ is also included.

Hamiltonian Effective Field Theory Model

- Consider the $\Lambda(1405)$.
- The four octet meson-baryon interaction channels of the $\Lambda(1405)$ are considered: $\pi\Sigma$, $\overline{K}N$, $K\Xi$ and $\eta\Lambda$.
- A single-particle state with bare mass, $m_0 + \alpha_0\, m_\pi^2$ is also included.
- In a finite periodic volume, momentum is quantised to $n\,(2\pi/L)$.

Hamiltonian Effective Field Theory Model

- Consider the $\Lambda(1405)$.
- The four octet meson-baryon interaction channels of the $\Lambda(1405)$ are considered: $\pi\Sigma$, $\overline{K}N$, $K\Xi$ and $\eta\Lambda$.
- A single-particle state with bare mass, $m_0 + \alpha_0\, m_\pi^2$ is also included.
- In a finite periodic volume, momentum is quantised to $n\,(2\pi/L)$.
- Working on a cubic volume of extent L on each side, it is convenient to define the momentum magnitudes

$$k_n = \sqrt{n_x^2 + n_y^2 + n_z^2}\,\frac{2\pi}{L}\,,$$

with $n_i = 0, 1, 2, \ldots$ and integer $n = n_x^2 + n_y^2 + n_z^2$.

Hamiltonian model, H_0

Denoting each meson-baryon energy by $\omega_{MB}(k_n) = \omega_M(k_n) + \omega_B(k_n)$, with $\omega_A(k_n) \equiv \sqrt{k_n^2 + m_A^2}$, the non-interacting Hamiltonian takes the form

$$H_0 = \begin{pmatrix} m_0 + \alpha_0\, m_\pi^2 & 0 & 0 & \cdots \\ 0 & \begin{matrix} \omega_{\pi\Sigma}(k_0) & \\ & \ddots \\ & & \omega_{\eta\Lambda}(k_0) \end{matrix} & 0 & \cdots \\ 0 & 0 & \begin{matrix} \omega_{\pi\Sigma}(k_1) & \\ & \ddots \\ & & \omega_{\eta\Lambda}(k_1) \end{matrix} & \cdots \\ \vdots & \vdots & \vdots & \ddots \end{pmatrix}.$$

Hamiltonian model, H_I

- Interaction entries describe the coupling of the single-particle state to the two-particle meson-baryon states.

Hamiltonian model, H_I

- Interaction entries describe the coupling of the single-particle state to the two-particle meson-baryon states.
- Each entry represents the S-wave interaction energy of the $\Lambda(1405)$ with one of the four channels at a certain value for k_n.

$$
H_I = \begin{pmatrix}
0 & g_{\pi\Sigma}(k_0) & \cdots & g_{\eta\Lambda}(k_0) & g_{\pi\Sigma}(k_1) & \cdots & g_{\eta\Lambda}(k_1)\cdots \\
g_{\pi\Sigma}(k_0) & 0 & \cdots & & & & \\
\vdots & \vdots & 0 & & & & \\
g_{\eta\Lambda}(k_0) & & & \ddots & & & \\
g_{\pi\Sigma}(k_1) & & & & & & \\
\vdots & & & & & & \\
g_{\eta\Lambda}(k_1) & & & & & & \\
\vdots & & & & & &
\end{pmatrix} .
$$

Eigenvalue Equation Form

- The eigenvalue equation corresponding to our Hamiltonian model is

$$\lambda = m_0 + \alpha_0\, m_\pi^2 - \sum_{M,B} \sum_{n=0}^{\infty} \frac{g_{MB}^2(k_n)}{\omega_{MB}(k_n) - \lambda}\,.$$

with λ denoting the energy eigenvalue.

Eigenvalue Equation Form

- The eigenvalue equation corresponding to our Hamiltonian model is

$$\lambda = m_0 + \alpha_0 \, m_\pi^2 - \sum_{M,B} \sum_{n=0}^{\infty} \frac{g_{MB}^2(k_n)}{\omega_{MB}(k_n) - \lambda} \, .$$

  with λ denoting the energy eigenvalue.
- As λ is finite, the pole in the denominator of the right-hand side is never accessed.
- The bare mass and the free meson-baryon energies encounter self-energy corrections that lead to avoided level-crossings in the finite-volume energy eigenstates.

Eigenvalue Equation Form

- The eigenvalue equation corresponding to our Hamiltonian model is

$$\lambda = m_0 + \alpha_0\, m_\pi^2 - \sum_{M,B} \sum_{n=0}^{\infty} \frac{g_{MB}^2(k_n)}{\omega_{MB}(k_n) - \lambda}\,.$$

  with λ denoting the energy eigenvalue.
- As λ is finite, the pole in the denominator of the right-hand side is never accessed.
- The bare mass and the free meson-baryon energies encounter self-energy corrections that lead to avoided level-crossings in the finite-volume energy eigenstates.
- Reference to chiral effective field theory provides the form of $g_{MB}(k_n)$.

Hamiltonian model solution and fit

- Flavour-singlet couplings between the bare state and the meson-baryon states are constrained by $SU(3)$-flavour symmetry and the width of the $\Lambda(1405)$ resonance.

Hamiltonian model solution and fit

- Flavour-singlet couplings between the bare state and the meson-baryon states are constrained by $SU(3)$-flavour symmetry and the width of the $\Lambda(1405)$ resonance.
- The eigenvalues and eigenvectors of H are obtained via the LAPACK software library.

Hamiltonian model solution and fit

- Flavour-singlet couplings between the bare state and the meson-baryon states are constrained by $SU(3)$-flavour symmetry and the width of the $\Lambda(1405)$ resonance.
- The eigenvalues and eigenvectors of H are obtained via the LAPACK software library.
- The bare mass parameters m_0 and α_0 are determined by a fit to the lattice QCD results.

Hamiltonian model fit

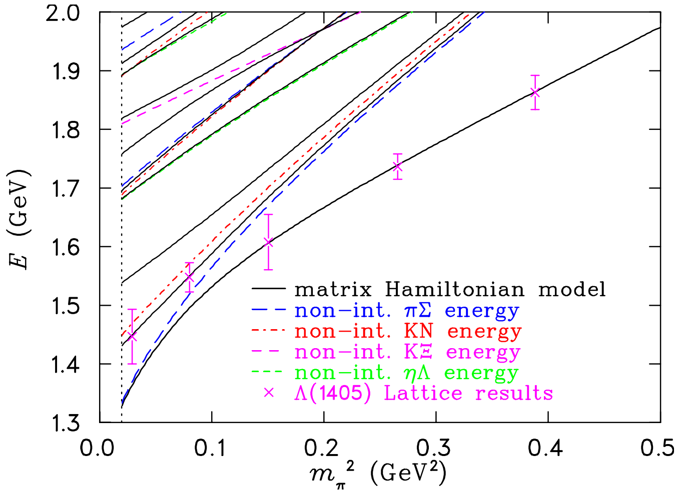

Avoided Level Crossing

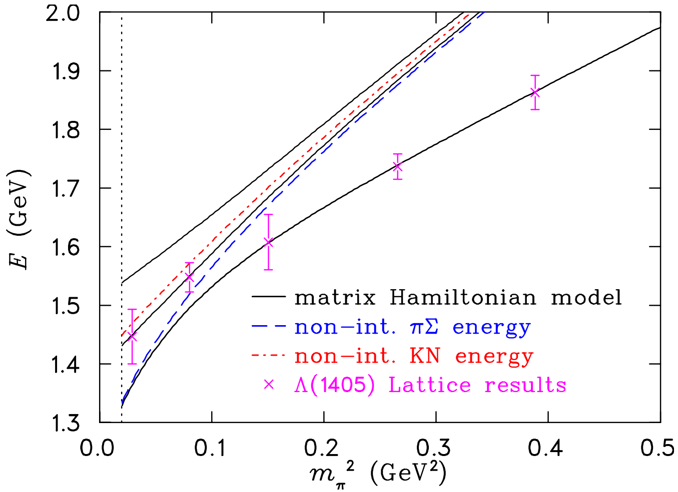

Energy eigenstate, $|E\rangle$, basis $|state\rangle$ composition

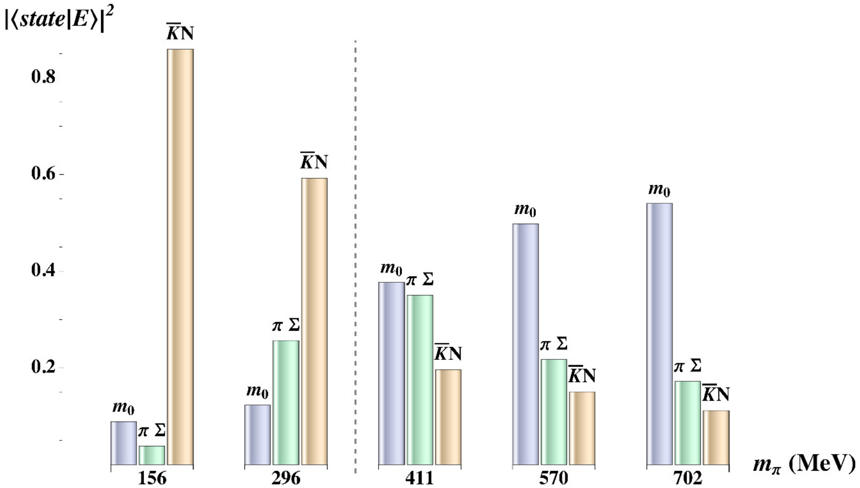

Hamiltonian model, H_I

- Our approach included a bare state dressed by flavour-singlet coupled meson-baryon channels

$$H_I = \begin{pmatrix} 0 & g_{\pi\Sigma}(k_0) & \cdots & g_{\eta\Lambda}(k_0) & g_{\pi\Sigma}(k_1) & \cdots & g_{\eta\Lambda}(k_1)\cdots \\ g_{\pi\Sigma}(k_0) & 0 & \cdots & & & & \\ \vdots & \vdots & 0 & & & & \\ & & & \ddots & & & \\ g_{\eta\Lambda}(k_0) & & & & & & \\ g_{\pi\Sigma}(k_1) & & & & & & \\ \vdots & & & & & & \\ g_{\eta\Lambda}(k_1) & & & & & & \\ \vdots & & & & & & \end{pmatrix} .$$

Hamiltonian model, H_I

- Our approach included a bare state dressed by flavour-singlet coupled meson-baryon channels

$$H_I = \begin{pmatrix} 0 & g_{\pi\Sigma}(k_0) & \cdots & g_{\eta\Lambda}(k_0) & g_{\pi\Sigma}(k_1) & \cdots & g_{\eta\Lambda}(k_1)\cdots \\ g_{\pi\Sigma}(k_0) & 0 & \cdots & & & & \\ \vdots & \vdots & 0 & & & & \\ & & & \ddots & & & \\ g_{\eta\Lambda}(k_0) & & & & & & \\ g_{\pi\Sigma}(k_1) & & & & & & \\ \vdots & & & & & & \\ g_{\eta\Lambda}(k_1) & & & & & & \\ \vdots & & & & & & \end{pmatrix} .$$

- Ironically, most analyses omit these interactions and instead include only the direct meson-baryon to meson-baryon interactions
    - Weinberg-Tomozawa terms

The two-pole description of the Λ(1405)

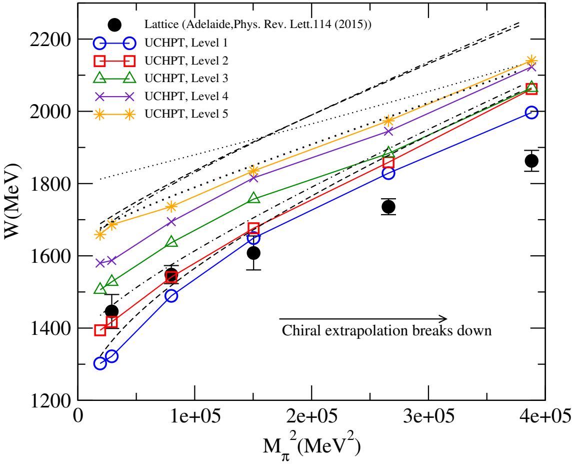

Raquel Molina and Michael Doring, arXiv:1512.05831 [hep-lat]

Direct two-to-two particle interactions

- We use the potential derived from Weinberg-Tomozawa term

$$V^{I}_{\alpha,\beta}(k,k') = \frac{g^{I}_{\alpha,\beta}}{8\pi^2 f_\pi^2} \frac{\omega_{\alpha_M}(k) + \omega_{\beta_M}(k')}{\sqrt{2\omega_{\alpha_M}(k)}\sqrt{2\omega_{\beta_M}(k')}} \, u(k)\, u(k')\,.$$

Direct two-to-two particle interactions

- We use the potential derived from Weinberg-Tomozawa term

$$V^{I}_{\alpha,\beta}(k,k') = \frac{g^{I}_{\alpha,\beta}}{8\pi^2 f_\pi^2} \frac{\omega_{\alpha_M}(k) + \omega_{\beta_M}(k')}{\sqrt{2\omega_{\alpha_M}(k)}\,\sqrt{2\omega_{\beta_M}(k')}}\, u(k)\, u(k')\,.$$

- Dipole regulator functions $u(k)$ have a fixed scale of $\Lambda = 1$ GeV.

Direct two-to-two particle interactions

- We use the potential derived from Weinberg-Tomozawa term

$$V^{I}_{\alpha,\beta}(k,k') = \frac{g^{I}_{\alpha,\beta}}{8\pi^2 f_\pi^2} \frac{\omega_{\alpha_M}(k) + \omega_{\beta_M}(k')}{\sqrt{2\omega_{\alpha_M}(k)}\,\sqrt{2\omega_{\beta_M}(k')}}\, u(k)\, u(k')\,.$$

- Dipole regulator functions $u(k)$ have a fixed scale of $\Lambda = 1$ GeV.
- Couplings vanishing in the $SU(3)$-flavour symmetry limit are not considered.

Direct two-to-two particle interactions

- Eight non-trivial couplings are constrained by experimental data in infinite volume.

$$g^0_{\pi\Sigma,\pi\Sigma},\ g^0_{\bar{K}N,\bar{K}N},\ g^0_{\bar{K}N,\pi\Sigma},\ g^0_{H},\ g^1_{\pi\Sigma,\pi\Sigma},\ g^1_{\bar{K}N,\bar{K}N},\ g^1_{\bar{K}N,\pi\Sigma},\ g^1_{\bar{K}N,\pi\Lambda},$$

with $SU(3)$ flavour symmetry constraints for the heavier $\eta\Lambda$ and $K\Xi$ channels

$$\begin{aligned} g^0_{\bar{K}N,\eta\Lambda} &= -3/\sqrt{2}\,g^0_H, \quad & g^0_{\pi\Sigma,K\Xi} &= -\sqrt{3/2}\,g^0_H, \\ g^0_{\eta\Lambda,K\Xi} &= 3/\sqrt{2}\,g^0_H, & g^0_{K\Xi,K\Xi} &= -3\,g^0_H. \end{aligned} \tag{1}$$

Direct two-to-two particle interactions

- Eight non-trivial couplings are constrained by experimental data in infinite volume.

$$g^0_{\pi\Sigma,\pi\Sigma},\; g^0_{\bar{K}N,\bar{K}N},\; g^0_{\bar{K}N,\pi\Sigma},\; g^0_{H},\; g^1_{\pi\Sigma,\pi\Sigma},\; g^1_{\bar{K}N,\bar{K}N},\; g^1_{\bar{K}N,\pi\Sigma},\; g^1_{\bar{K}N,\pi\Lambda},$$

  with $SU(3)$ flavour symmetry constraints for the heavier $\eta\Lambda$ and $K\Xi$ channels

$$\begin{aligned} g^0_{\bar{K}N,\eta\Lambda} &= -3/\sqrt{2}\,g^0_H, \quad & g^0_{\pi\Sigma,K\Xi} &= -\sqrt{3/2}\,g^0_H, \\ g^0_{\eta\Lambda,K\Xi} &= 3/\sqrt{2}\,g^0_H, & g^0_{K\Xi,K\Xi} &= -3\,g^0_H. \end{aligned} \tag{1}$$

- Finite volume spectrum is then a prediction.

Couplings Constrained by Experiment

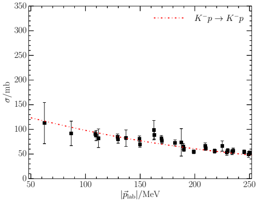

(a) $K^-p \to K^-p$

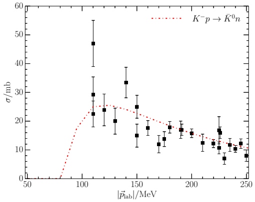

(b) $K^-p \to \bar{K}^0 n$

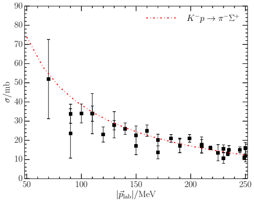

(c) $K^-p \to \pi^-\Sigma^+$

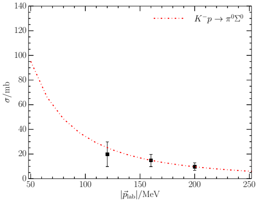

(d) $K^-p \to \pi^0\Sigma^0$

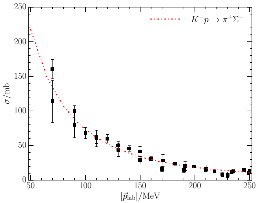

(e) $K^-p \to \pi^+\Sigma^-$

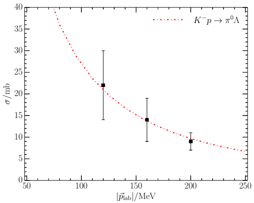

(f) $K^-p \to \pi^0\Lambda$

Finite Volume Λ Spectrum for $L = 3$ fm

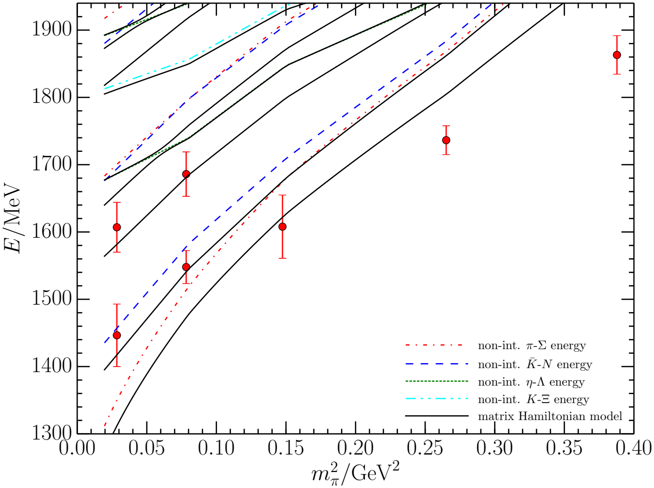

Comparison with UχPT

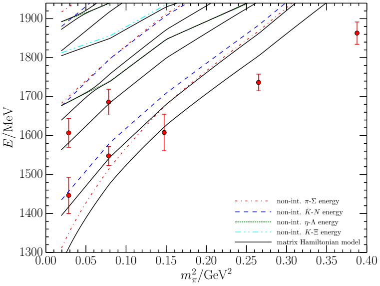

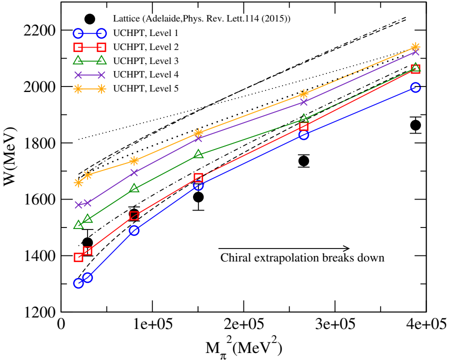

Raquel Molina and Michael Doring, arXiv:1512.05831 [hep-lat]

Direct two-to-two particle interactions & bare state

- Dipole regulator functions $u(k)$ have a fixed scale of $\Lambda = 1$ GeV.
- Same eight two-to-two particle couplings are considered

$$g^0_{\pi\Sigma,\pi\Sigma},\; g^0_{\bar{K}N,\bar{K}N},\; g^0_{\bar{K}N,\pi\Sigma},\; g^0_{H},\; g^1_{\pi\Sigma,\pi\Sigma},\; g^1_{\bar{K}N,\bar{K}N},\; g^1_{\bar{K}N,\pi\Sigma},\; g^1_{\bar{K}N,\pi\Lambda},$$

Direct two-to-two particle interactions & bare state

- Dipole regulator functions $u(k)$ have a fixed scale of $\Lambda = 1$ GeV.
- Same eight two-to-two particle couplings are considered

$$g^0_{\pi\Sigma,\pi\Sigma},\ g^0_{\bar{K}N,\bar{K}N},\ g^0_{\bar{K}N,\pi\Sigma},\ g^0_{H},\ g^1_{\pi\Sigma,\pi\Sigma},\ g^1_{\bar{K}N,\bar{K}N},\ g^1_{\bar{K}N,\pi\Sigma},\ g^1_{\bar{K}N,\pi\Lambda},$$

- Five new parameters describing bare to two-particle interactions are introduced

$$m^0_B,\ g^0_{\pi\Sigma,B_0},\ g^0_{\bar{K}N,B_0},\ g^0_{\eta\Lambda,B_0},\ g^0_{K\Xi,B_0},$$

Direct two-to-two particle interactions & bare state

- Dipole regulator functions $u(k)$ have a fixed scale of $\Lambda = 1$ GeV.
- Same eight two-to-two particle couplings are considered

$$g^0_{\pi\Sigma,\pi\Sigma},\ g^0_{\bar{K}N,\bar{K}N},\ g^0_{\bar{K}N,\pi\Sigma},\ g^0_{H},\ g^1_{\pi\Sigma,\pi\Sigma},\ g^1_{\bar{K}N,\bar{K}N},\ g^1_{\bar{K}N,\pi\Sigma},\ g^1_{\bar{K}N,\pi\Lambda},$$

- Five new parameters describing bare to two-particle interactions are introduced

$$m^0_B,\ g^0_{\pi\Sigma,B_0},\ g^0_{\bar{K}N,B_0},\ g^0_{\eta\Lambda,B_0},\ g^0_{K\Xi,B_0},$$

- These 13 parameters are constrained by experimental data.

Direct two-to-two particle interactions & bare state

- Dipole regulator functions $u(k)$ have a fixed scale of $\Lambda = 1$ GeV.
- Same eight two-to-two particle couplings are considered

$$g^0_{\pi\Sigma,\pi\Sigma},\ g^0_{\bar{K}N,\bar{K}N},\ g^0_{\bar{K}N,\pi\Sigma},\ g^0_{H},\ g^1_{\pi\Sigma,\pi\Sigma},\ g^1_{\bar{K}N,\bar{K}N},\ g^1_{\bar{K}N,\pi\Sigma},\ g^1_{\bar{K}N,\pi\Lambda},$$

- Five new parameters describing bare to two-particle interactions are introduced

$$m^0_B,\ g^0_{\pi\Sigma,B_0},\ g^0_{\bar{K}N,B_0},\ g^0_{\eta\Lambda,B_0},\ g^0_{K\Xi,B_0},$$

- These 13 parameters are constrained by experimental data.
- A linear quark mass dependence for the bare mass is constrained by the lattice results.

Couplings and m_B^0 Constrained by Experiment

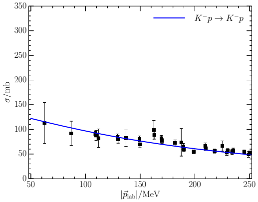

(a) $K^- p \to K^- p$

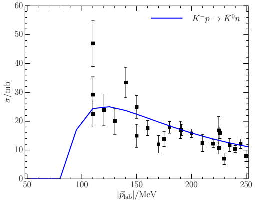

(b) $K^- p \to \bar{K}^0 n$

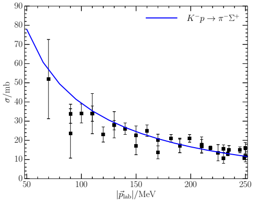

(c) $K^- p \to \pi^- \Sigma^+$

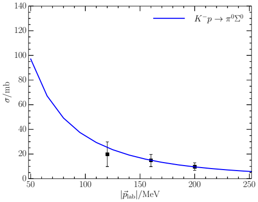

(d) $K^- p \to \pi^0 \Sigma^0$

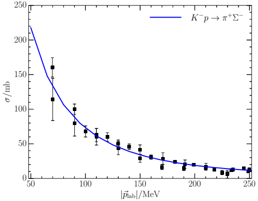

(e) $K^- p \to \pi^+ \Sigma^-$

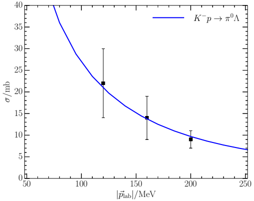

(f) $K^- p \to \pi^0 \Lambda$

Couplings and m_B^0 Constrained by Experiment

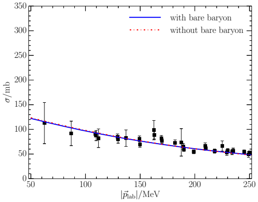

(a) $K^-p \to K^-p$

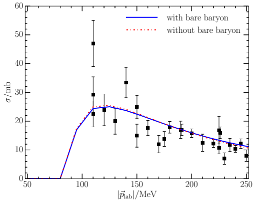

(b) $K^-p \to \bar{K}^0 n$

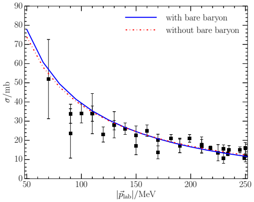

(c) $K^-p \to \pi^-\Sigma^+$

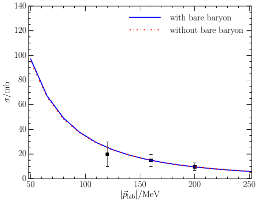

(d) $K^-p \to \pi^0\Sigma^0$

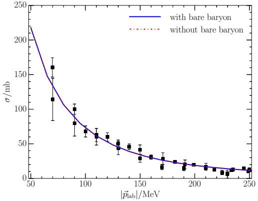

(e) $K^-p \to \pi^+\Sigma^-$

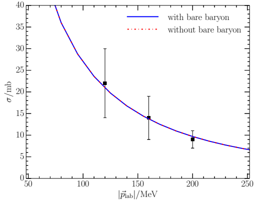

(f) $K^-p \to \pi^0\Lambda$

$I = 0$ Parameters		No Bare State	With Bare State
$g^0_{\pi\Sigma,\pi\Sigma}$		-1.77	-1.11
$g^0_{\bar{K}N,\bar{K}N}$		-2.14	-1.74
$g^0_{\bar{K}N,\pi\Sigma}$		0.78	1.26
g^0_H		0.20	0.46
$g^0_{\pi\Sigma,B_0}$		-	0.11
$g^0_{\bar{K}N,B_0}$		-	0.15
$g^0_{\eta\Lambda,B_0}$		-	-0.17
$g^0_{K\Xi,B_0}$		-	-0.08
m^0_B/MeV		-	1714
$\chi^2/$ (120 data)	UχPT	166	177
Pole 1 (MeV)	$1379 - i\,71$	$1333 - i\,85$	$1338 - i\,89$
Pole 2 (MeV)	$1412 - i\,20$	$1428 - i\,23$	$1430 - i\,22$

Finite Volume Λ Spectrum for $L = 3$ fm

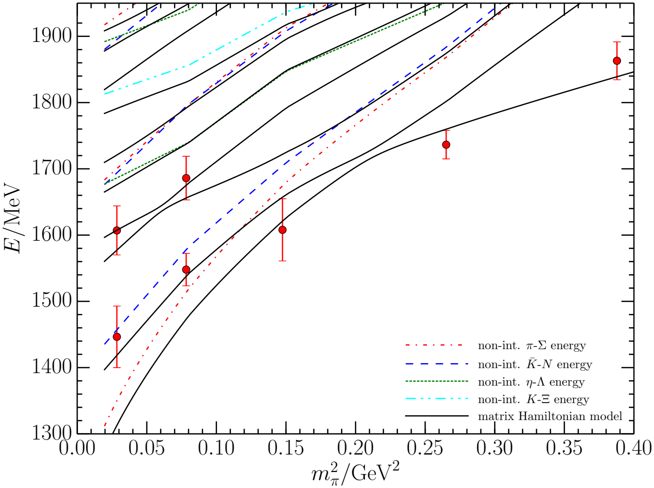

Finite Volume Λ Spectrum for $L = 3$ fm

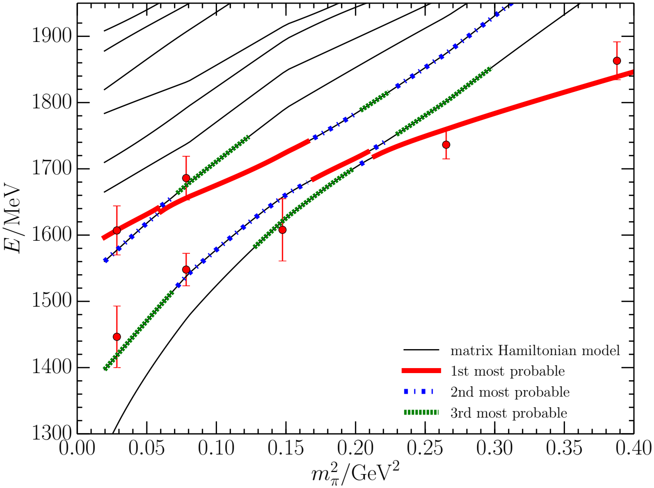

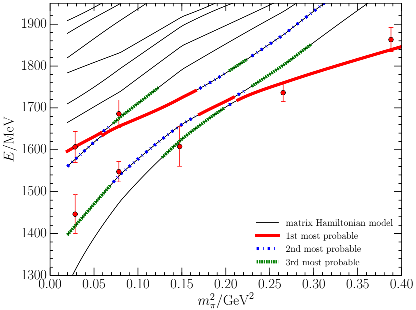

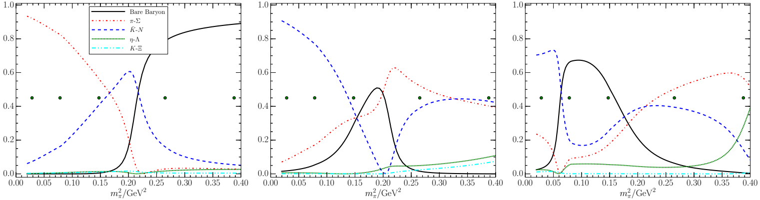

(a) State 1 (b) State 2 (c) State 3

Finite Volume Λ Spectrum for $L = 3$ fm

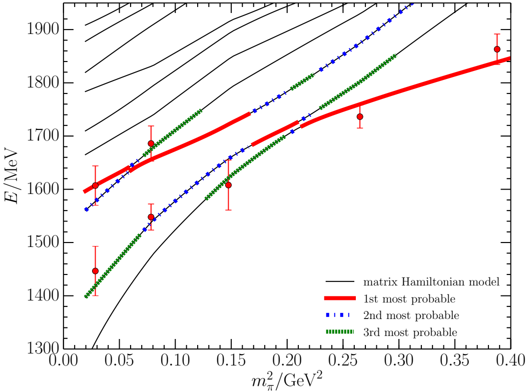

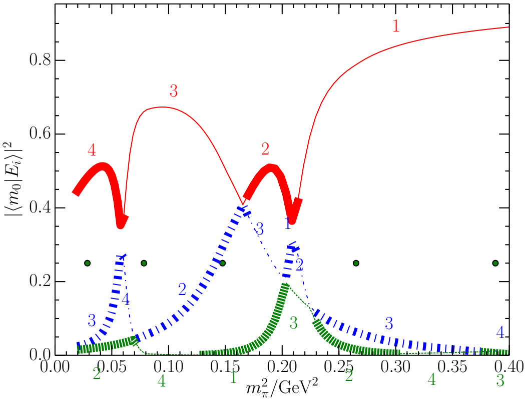

Conclusions - $\Lambda(1405)$ Resonance

- Lattice QCD calculations have revealed there are
  - No low-lying three-quark dominated states in the $\Lambda(1405)$ Resonance mass region.
  - Three-quark dominated states are associated with the octet states.

Conclusions - $\Lambda(1405)$ Resonance

- Lattice QCD calculations have revealed there are
  - No low-lying three-quark dominated states in the $\Lambda(1405)$ Resonance mass region.
  - Three-quark dominated states are associated with the octet states.
- $\Lambda(1405)$ structure is dominated by a $\overline{K}N$ molecule. Signified by:
  - The vanishing of the strange quark contribution to the magnetic moment of the $\Lambda(1405)$, and
  - The dominance of the $\overline{K}N$ component in finite-volume EFT.

Conclusions - $\Lambda(1405)$ Resonance

- Lattice QCD calculations have revealed there are
  - No low-lying three-quark dominated states in the $\Lambda(1405)$ Resonance mass region.
  - Three-quark dominated states are associated with the octet states.
- $\Lambda(1405)$ structure is dominated by a $\overline{K}N$ molecule. Signified by:
  - The vanishing of the strange quark contribution to the magnetic moment of the $\Lambda(1405)$, and
  - The dominance of the $\overline{K}N$ component in finite-volume EFT.
- The three-quark flavour-singlet $\Lambda(1405)$ anticipated by the quark model exists only at quark masses approaching the strange quark mass.

Low-lying negative-parity N^* Spectrum

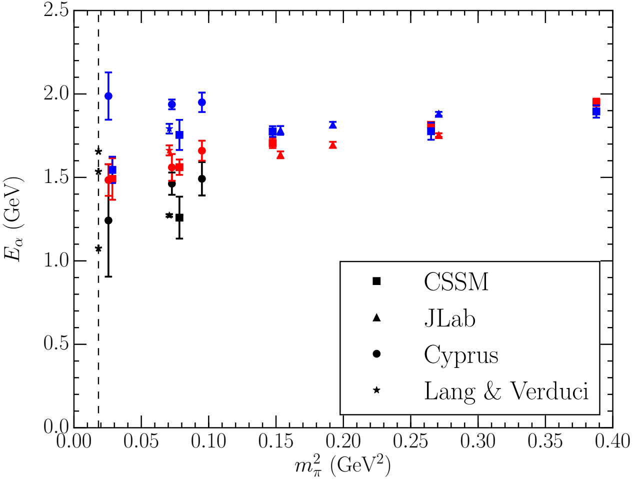

Constrain model parameters to experimental data

- Consider πN and ηN and bare state interactions.
- Fit to phase shift and inelasticity

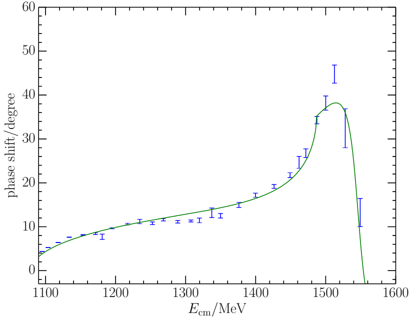

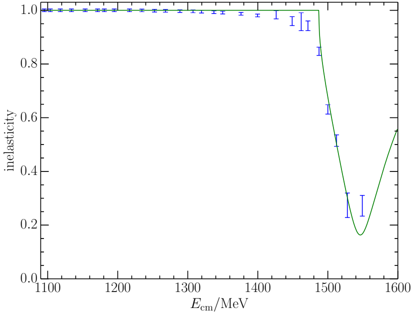

- Fit yields a pole at $1531 \pm 29 - i\,88 \pm 2$ MeV.
- Compare PDG estimate $1510 \pm 20 - i\,85 \pm 40$ MeV.

Hamiltonian Model N^* Spectrum: 2 fm

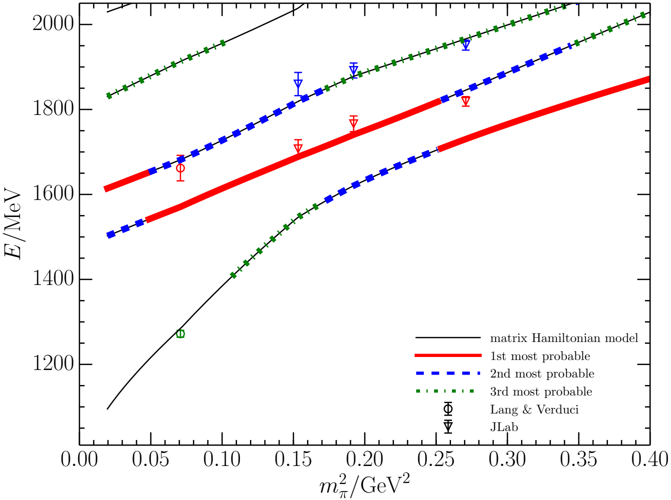

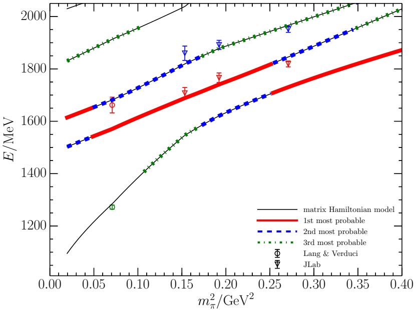

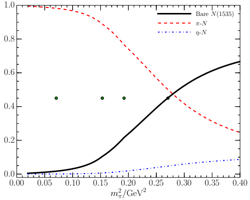

(a) State 1

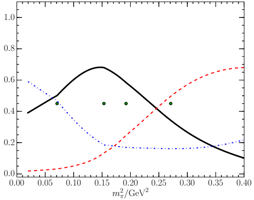

(b) State 2

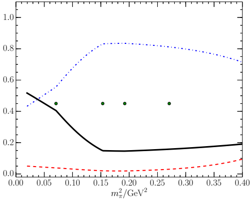

(c) State 3

Hamiltonian Model N^* Spectrum: 2 fm

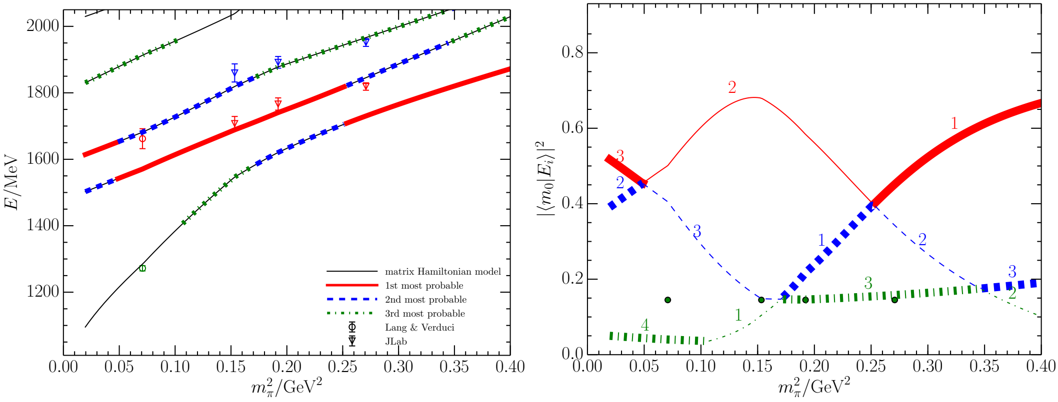

Hamiltonian Model N^* Spectrum: 3 fm

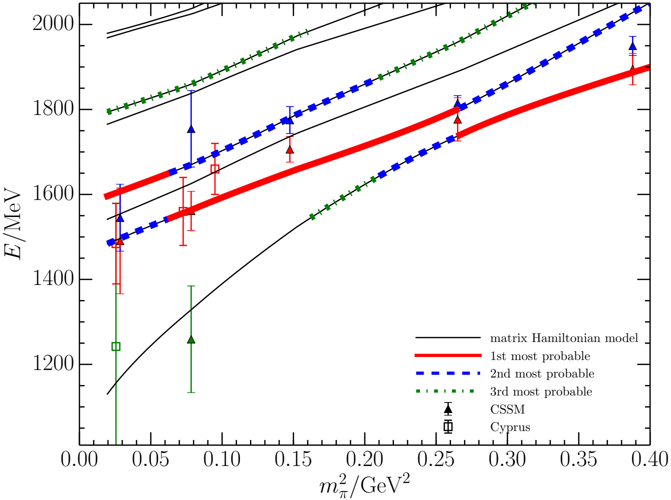

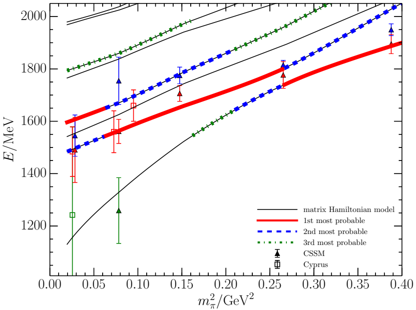

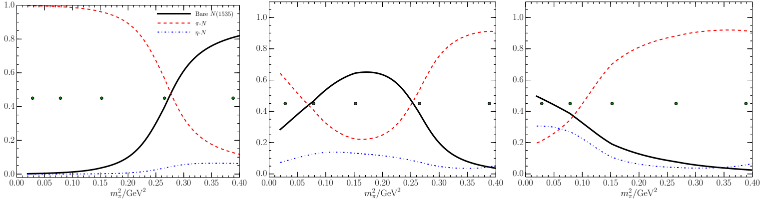

(a) State 1 (b) State 2 (c) State 4

Hamiltonian Model N^* Spectrum: 3 fm

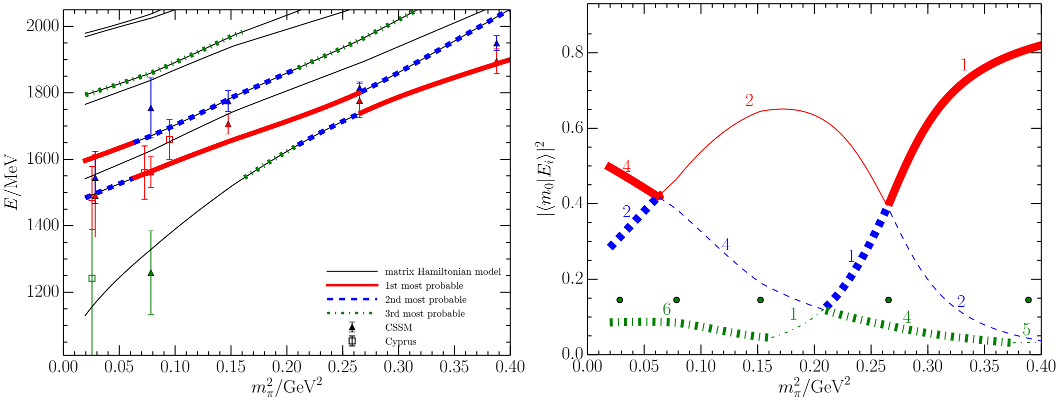

Conclusions - Odd-Parity Nucleon Resonances

- Lattice QCD calculations have revealed there are
  - Two low-lying states in the $N(1535)$ and $N(1650)$ resonance mass regions with large bare three-quark basis components.
  - These components compose $\sim 50\%$ of the states at the physical quark masses.

Conclusions - Odd-Parity Nucleon Resonances

- Lattice QCD calculations have revealed there are
  - Two low-lying states in the $N(1535)$ and $N(1650)$ resonance mass regions with large bare three-quark basis components.
  - These components compose $\sim 50\%$ of the states at the physical quark masses.
- ηN contributions dominate the meson-baryon dressings of these states.

Conclusions - Odd-Parity Nucleon Resonances

- Lattice QCD calculations have revealed there are
  - Two low-lying states in the $N(1535)$ and $N(1650)$ resonance mass regions with large bare three-quark basis components.
  - These components compose $\sim 50\%$ of the states at the physical quark masses.
- ηN contributions dominate the meson-baryon dressings of these states.
- Strong single-particle components make these states ideal for lattice studies of the form factors and transition moments.

Conclusions - Odd-Parity Nucleon Resonances

- Lattice QCD calculations have revealed there are
  - Two low-lying states in the $N(1535)$ and $N(1650)$ resonance mass regions with large bare three-quark basis components.
  - These components compose $\sim 50\%$ of the states at the physical quark masses.
- ηN contributions dominate the meson-baryon dressings of these states.
- Strong single-particle components make these states ideal for lattice studies of the form factors and transition moments.
- The lattice scattering state energy calculated by Lang and Verduci is described accurately by Hamiltonian effective field theory constrained to experiment.
  - Two-to-two particle meson-baryon interactions are essential to describing the lattice results.

What about the Roper? Lattice results at $L \simeq 3$ fm

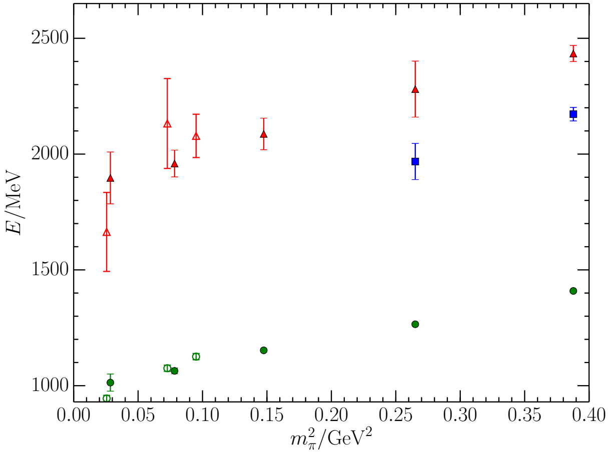

- Filled Symbols: CSSM

Open Symbols: Cyprus Collaboration

What about the Roper? Lattice results at $L \simeq 3$ fm

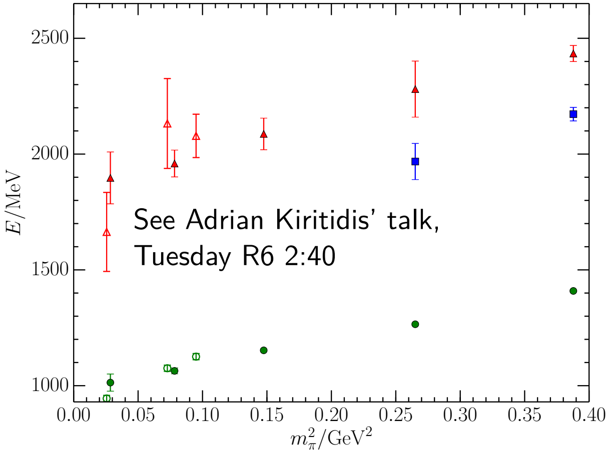

- Filled Symbols: CSSM

Open Symbols: Cyprus Collaboration

Athens Model Independent Analysis Scheme (AMIAS)

- “Novel analysis method for excited states in lattice QCD:
  The nucleon case,”
  C. Alexandrou, T. Leontiou, C. N. Papanicolas and E. Stiliaris,
  Phys. Rev. D **91** (2015) 1, 014506
  arXiv:1411.6765 [hep-lat].

Bare Roper Case: $m_0 = 2.03$ GeV

- Consider πN, $\pi\Delta$ and σN channels, dressing a bare state.
- Fit to phase shift and inelasticity

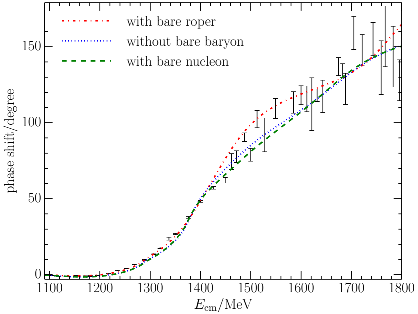

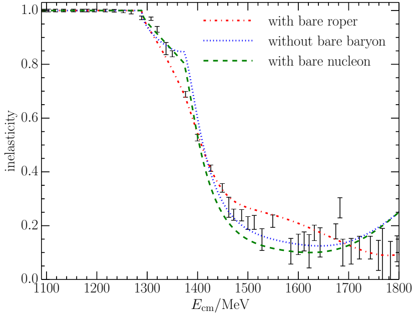

- Fit yields a pole at $1380 - i\,87$ MeV.
- Compare PDG estimate $1365 \pm 15 - i\,95 \pm 15$ MeV.

Bare Roper: Hamiltonian Model N' Spectrum

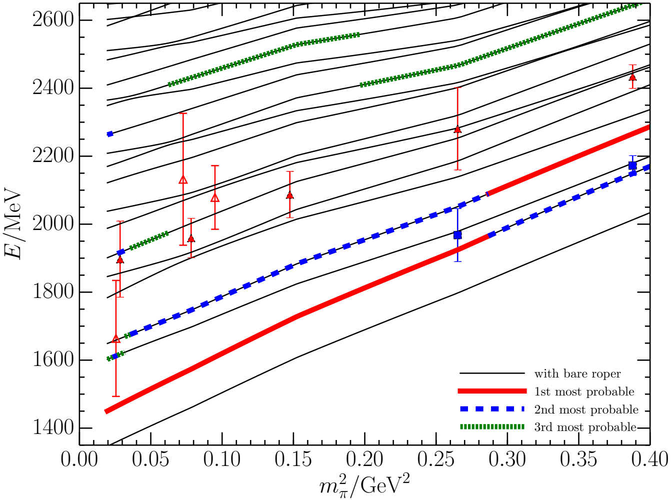

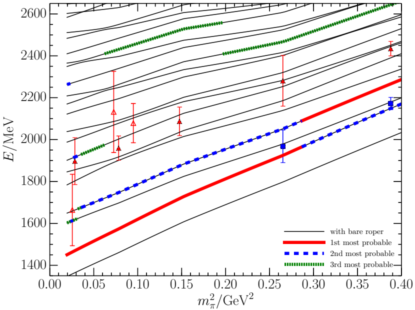

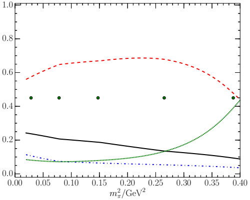

(a) State 2

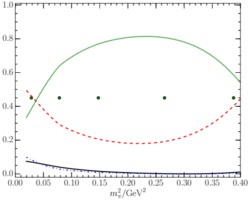

(b) State 3

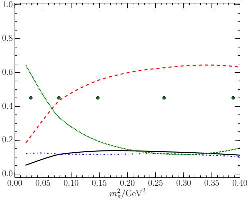

(c) State 4

Bare Roper: Hamiltonian Model N' Spectrum

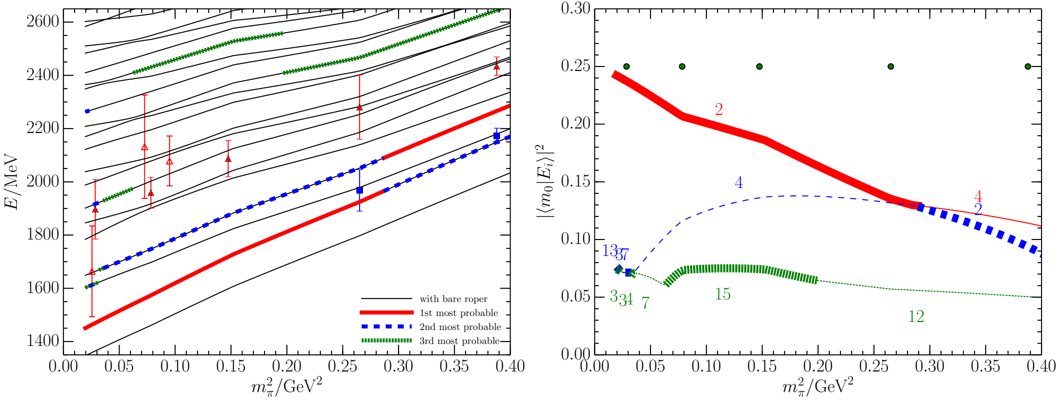

Bare Nucleon Case: $m_0 = 1.17$ GeV

- Consider πN, $\pi\Delta$ and σN channels, dressing a bare state.
- Fit to phase shift and inelasticity

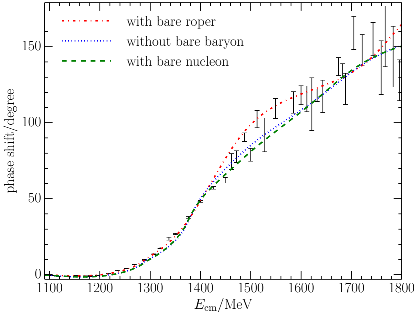

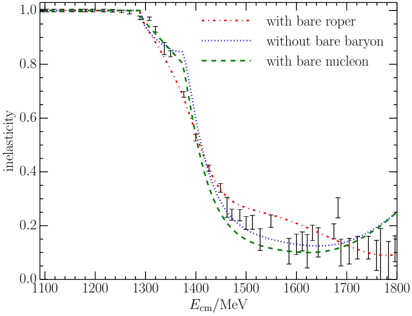

- Fit yields a pole at 1357 $- i\,36$ MeV.
- Compare PDG estimate $1365 \pm 15 - i\,95 \pm 15$ MeV.

Bare Nucleon: Hamiltonian Model N' Spectrum

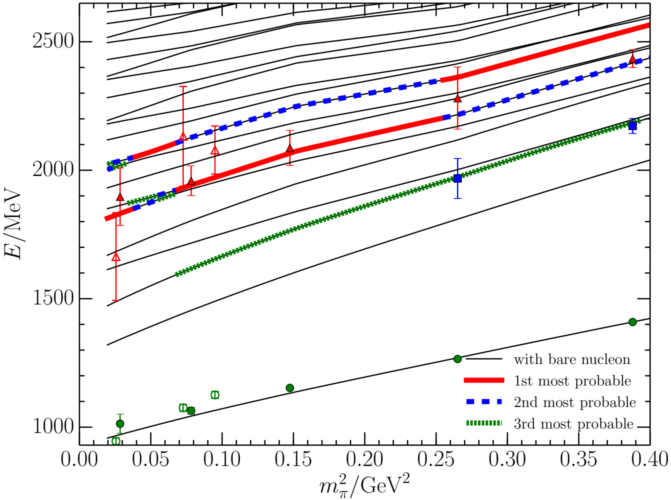

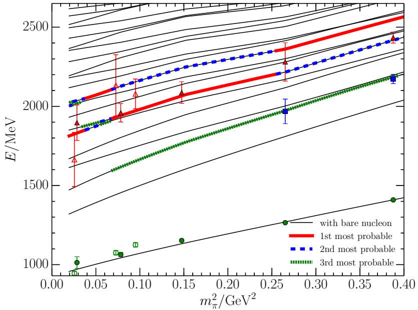

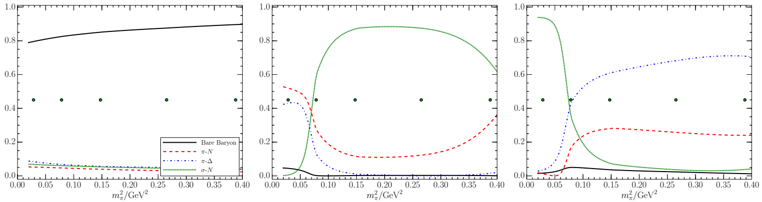

(a) State 1 (b) State 6 (c) State 7

Bare Nucleon: Hamiltonian Model N' Spectrum

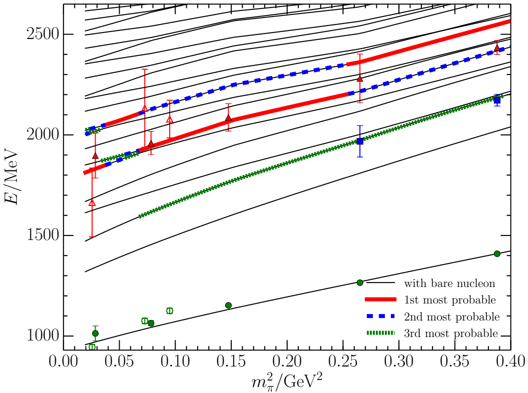

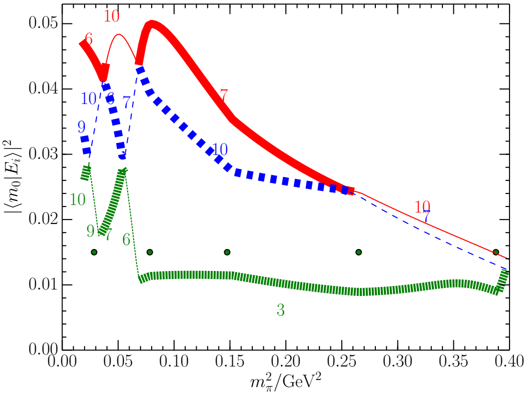

Conclusions - Roper Resonance

- Lattice QCD calculations have revealed there are
  - No low-lying three-quark dominated states in the Roper Resonance mass region.
  - No localised meson-baryon states at light quark masses.

Conclusions - Roper Resonance

- Lattice QCD calculations have revealed there are
  - No low-lying three-quark dominated states in the Roper Resonance mass region.
  - No localised meson-baryon states at light quark masses.
- Roper of the Constituent Quark Model has been seen on the lattice.
  - Node structure and density is similar to model expectations.

Conclusions - Roper Resonance

- Lattice QCD calculations have revealed there are
  - No low-lying three-quark dominated states in the Roper Resonance mass region.
  - No localised meson-baryon states at light quark masses.
- Roper of the Constituent Quark Model has been seen on the lattice.
  - Node structure and density is similar to model expectations.
- Hamiltonian Effective field theory explains the states observed in Lattice QCD as
  - Having a small three-quark component associated with a light bare-nucleon basis state.

Conclusions - Roper Resonance

- Lattice QCD calculations have revealed there are
  - No low-lying three-quark dominated states in the Roper Resonance mass region.
  - No localised meson-baryon states at light quark masses.
- Roper of the Constituent Quark Model has been seen on the lattice.
  - Node structure and density is similar to model expectations.
- Hamiltonian Effective field theory explains the states observed in Lattice QCD as
  - Having a small three-quark component associated with a light bare-nucleon basis state.
- Like the $\Lambda(1405)$, the Roper resonance is dominated by meson-baryon degrees of freedom.

Conclusions - Roper Resonance

- Lattice QCD calculations have revealed there are
  - No low-lying three-quark dominated states in the Roper Resonance mass region.
  - No localised meson-baryon states at light quark masses.
- Roper of the Constituent Quark Model has been seen on the lattice.
  - Node structure and density is similar to model expectations.
- Hamiltonian Effective field theory explains the states observed in Lattice QCD as
  - Having a small three-quark component associated with a light bare-nucleon basis state.
- Like the $\Lambda(1405)$, the Roper resonance is dominated by meson-baryon degrees of freedom.
- Conclude that the Roper Resonance is dynamically generated
  - dominated by the direct two-to-two particle meson-baryon interactions.

Artistic view of $\Lambda(1405)$ Structure

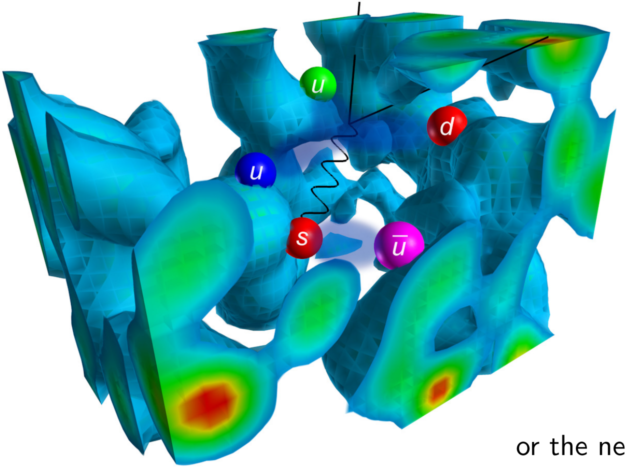

or the neutral Roper upon $s \to d$.

Supplementary Information

The following slides provide additional information which may be of interest.

Variational Analysis

- Consider a basis of interpolating fields χ_i

Variational Analysis

- Consider a basis of interpolating fields χ_i
- Construct the correlation matrix

$$
\begin{aligned}
G_{ij}(\mathbf{p};t) &= \sum_{\mathbf{x}} \mathrm{e}^{-\mathrm{i}\,\mathbf{p}\cdot\mathbf{x}}\,\mathrm{tr}\left(\Gamma\,\langle\Omega|\,\chi_i(x)\,\overline{\chi}_j(0)\,|\Omega\rangle\right) \\
&= \sum_{\alpha} A_i^{\alpha}\,A_j^{\dagger\alpha}\,\exp\left(-E_{\alpha}(\mathbf{p})\,t\right)\,.
\end{aligned}
$$

Variational Analysis

- Consider a basis of interpolating fields χ_i
- Construct the correlation matrix

$$
\begin{aligned}
G_{ij}(\mathbf{p};t) &= \sum_{\mathbf{x}} \mathrm{e}^{-\mathrm{i}\,\mathbf{p}\cdot\mathbf{x}}\,\mathrm{tr}\left(\Gamma\,\langle\Omega|\,\chi_i(x)\,\overline{\chi}_j(0)\,|\Omega\rangle\right) \\
&= \sum_{\alpha} A_i^{\alpha}\,A_j^{\dagger\alpha}\,\exp\left(-E_\alpha(\mathbf{p})\,t\right)\,.
\end{aligned}
$$

- Seek linear combinations of the interpolators $\{\,\chi_i\,\}$ that isolate individual energy eigenstates, α, at momentum $\mathbf{p}$:

$$
\phi^{\alpha} = v_i^{\alpha}(\mathbf{p})\,\chi_i\,, \qquad \overline{\phi}^{\alpha} = u_i^{\alpha}(\mathbf{p})\,\overline{\chi}_i\,.
$$

Variational Analysis

- When successful, only state α participates in the correlation function, and one can write recurrence relations

$$G(\mathbf{p}; t_0 + \delta t)\, \mathbf{u}^{\alpha}(\mathbf{p}) = \mathrm{e}^{-E_{\alpha}(\mathbf{p})\,\delta t}\, G(\mathbf{p}; t_0)\, \mathbf{u}^{\alpha}(\mathbf{p})$$

$$\mathbf{v}^{\alpha\,\mathsf{T}}(\mathbf{p})\, G(\mathbf{p}; t_0 + \delta t) = \mathrm{e}^{-E_{\alpha}(\mathbf{p})\,\delta t}\, \mathbf{v}^{\alpha\,\mathsf{T}}(\mathbf{p})\, G(\mathbf{p}; t_0)$$

a Generalised Eigenvalue Problem (GEVP).

Variational Analysis

- When successful, only state α participates in the correlation function, and one can write recurrence relations

$$G(\mathbf{p}; t_0 + \delta t)\, \mathbf{u}^{\alpha}(\mathbf{p}) = e^{-E_{\alpha}(\mathbf{p})\,\delta t}\, G(\mathbf{p}; t_0)\, \mathbf{u}^{\alpha}(\mathbf{p})$$

$$\mathbf{v}^{\alpha\mathsf{T}}(\mathbf{p})\, G(\mathbf{p}; t_0 + \delta t) = e^{-E_{\alpha}(\mathbf{p})\,\delta t}\, \mathbf{v}^{\alpha\mathsf{T}}(\mathbf{p})\, G(\mathbf{p}; t_0)$$

  a Generalised Eigenvalue Problem (GEVP).

- Solve for the left, $\mathbf{v}^{\alpha}(\mathbf{p})$, and right, $\mathbf{u}^{\alpha}(\mathbf{p})$, generalised eigenvectors of $G(\mathbf{p}; t_0 + \delta t)$ and $G(\mathbf{p}; t_0)$.

Eigenstate-Projected Correlation Functions

- Using these optimal eigenvectors, create eigenstate-projected correlation functions

$$
\begin{aligned}
G^{\alpha}(\mathbf{p};t) &= \sum_{\mathbf{x}} \mathrm{e}^{-\mathrm{i}\,\mathbf{p}\cdot\mathbf{x}} \left\langle \Omega \middle| \phi^{\alpha}(x)\, \overline{\phi}^{\alpha}(0) \middle| \Omega \right\rangle \,, \\
&= \sum_{\mathbf{x}} \mathrm{e}^{-\mathrm{i}\,\mathbf{p}\cdot\mathbf{x}} \left\langle \Omega \middle| v_i^{\alpha}(\mathbf{p})\, \chi_i(x)\, \overline{\chi}_j(0)\, u_j^{\alpha}(\mathbf{p}) \middle| \Omega \right\rangle \,, \\
&= \mathbf{v}^{\alpha\,\mathsf{T}}(\mathbf{p})\, G(\mathbf{p};t)\, \mathbf{u}^{\alpha}(\mathbf{p}) \,.
\end{aligned}
$$

$$
G^{\alpha}(\mathbf{p};t) = A_{\alpha}\, \exp\left(-E_{\alpha}(\mathbf{p})\, t\right) \,.
$$

Eigenstate-Projected Correlation Functions

- Using these optimal eigenvectors, create eigenstate-projected correlation functions

$$
\begin{aligned}
G^{\alpha}(\mathbf{p};t) &= \sum_{\mathbf{x}} \mathrm{e}^{-\mathrm{i}\,\mathbf{p}\cdot\mathbf{x}} \, \langle \Omega | \phi^{\alpha}(x) \, \overline{\phi}^{\alpha}(0) | \Omega \rangle \ , \\
&= \sum_{\mathbf{x}} \mathrm{e}^{-\mathrm{i}\,\mathbf{p}\cdot\mathbf{x}} \, \langle \Omega | v_i^{\alpha}(\mathbf{p}) \, \chi_i(x) \, \overline{\chi}_j(0) \, u_j^{\alpha}(\mathbf{p}) | \Omega \rangle \ , \\
&= \mathbf{v}^{\alpha \mathsf{T}}(\mathbf{p}) \, G(\mathbf{p};t) \, \mathbf{u}^{\alpha}(\mathbf{p}) \, .
\end{aligned}
$$

$$
G^{\alpha}(\mathbf{p};t) = A_{\alpha} \, \exp\left(-E_{\alpha}(\mathbf{p}) \, t\right) \ .
$$

- Here t is different from t_0 and δt and can become large.

Smeared Source to Point Sink Correlation Functions

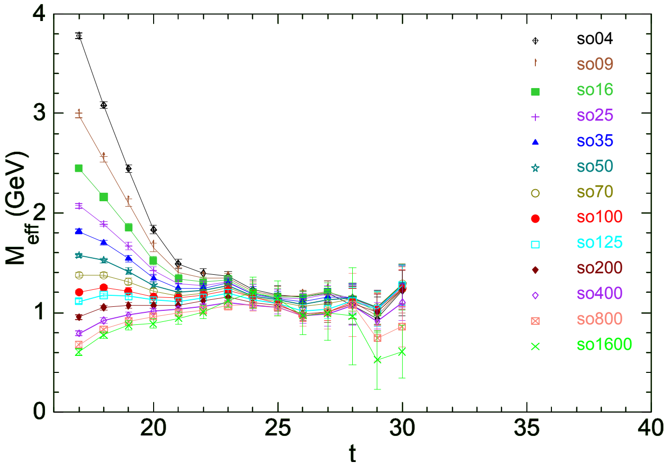

States Tracked via Orthogonal Eigenvectors

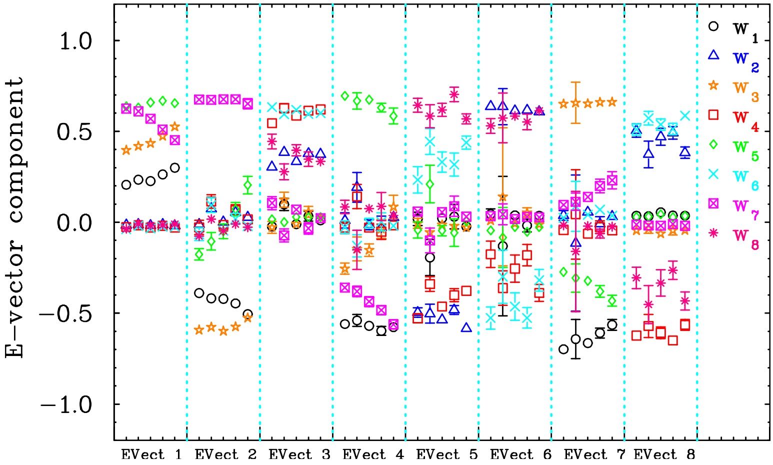

Positive Parity Nucleon Spectrum: CSSM

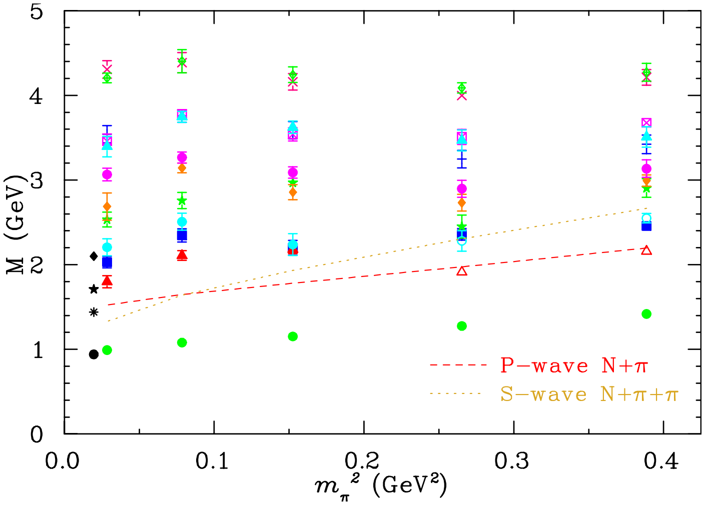

Further Information

- "Roper Resonance in 2+1 Flavor QCD,"
  M. S. Mahbub, *et al.* [CSSM],
  Phys. Lett. B **707** (2012) 389
  arXiv:1011.5724 [hep-lat],

- "Low-lying Odd-parity States of the Nucleon in Lattice QCD,"
  M. Selim Mahbub, *et al.* [CSSM],
  Phys. Rev. D Rapid Comm. **87** (2013) 011501,
  arXiv:1209.0240 [hep-lat]

- "Structure and Flow of the Nucleon Eigenstates in Lattice QCD,"
  M. S. Mahbub, *et al.* [CSSM],
  Phys. Rev. D **87** (2013) 9, 094506
  arXiv:1302.2987 [hep-lat].

Sequential Empirical Bayesian (SEB) Analysis: χQCD Collaboration

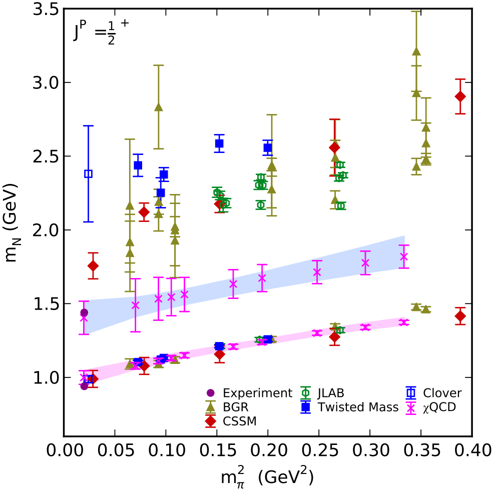

χQCD & HSC Systematic Comparison - Same Correlators Examined

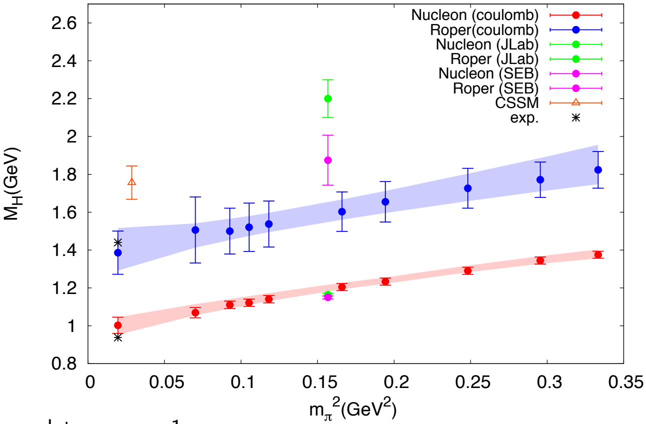

Note: $28 \times 28 = 784$ correlators versus 1.

K. F. Liu, *et. al*,PoS LATTICE **2013** (2014) 507, arXiv:1403.6847 [hep-ph]

Positive Parity Spectrum: Cyprus (Twisted Mass) Collaboration: Feb. '13

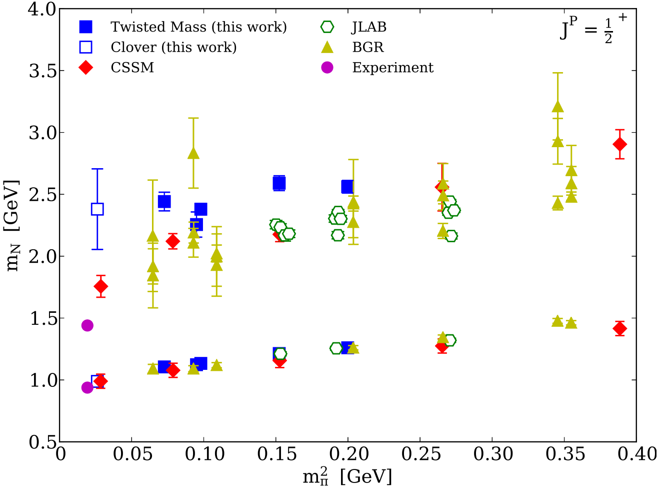

Positive Parity Spectrum: Cyprus (Twisted Mass) Collaboration: Jan. '14

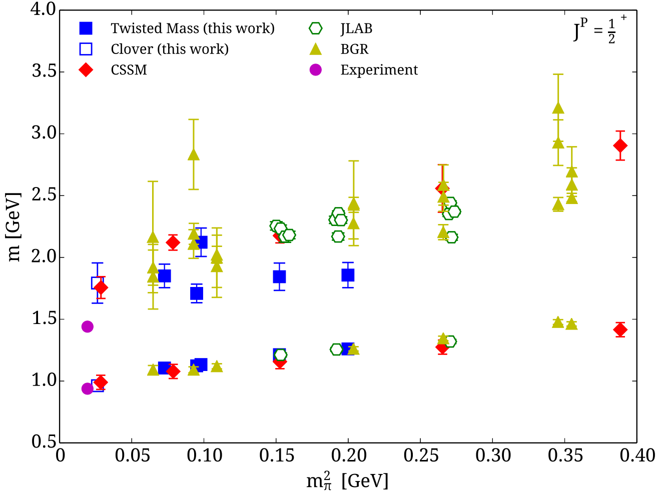

d-quark probability density in ground state proton: $m_\pi = 156$ MeV (CSSM)

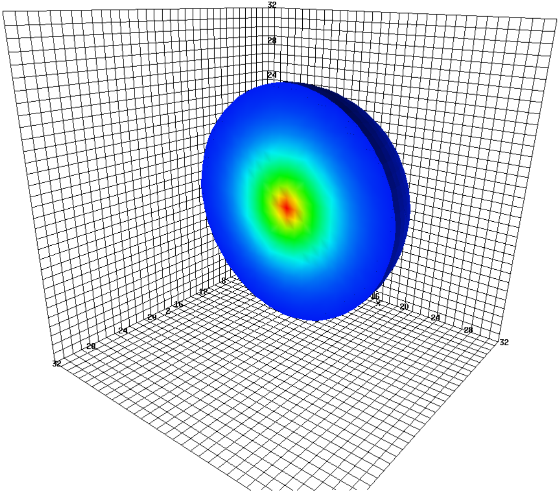

d-quark probability density in first excited proton: $m_\pi = 156$ MeV (CSSM)

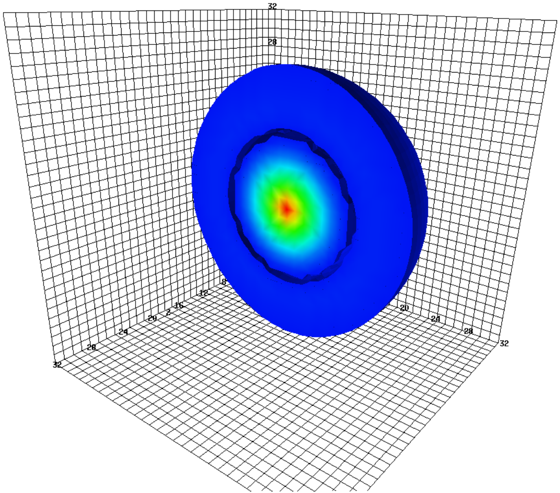

Positive Parity Nucleon Spectrum: only small smearing: Cyprus

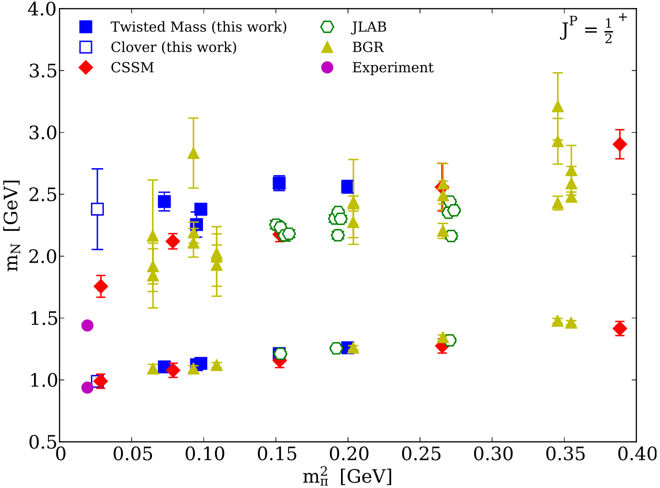

Positive Parity Nucleon Spectrum: r_{RMS} smearing of 8.6 lu: Cyprus

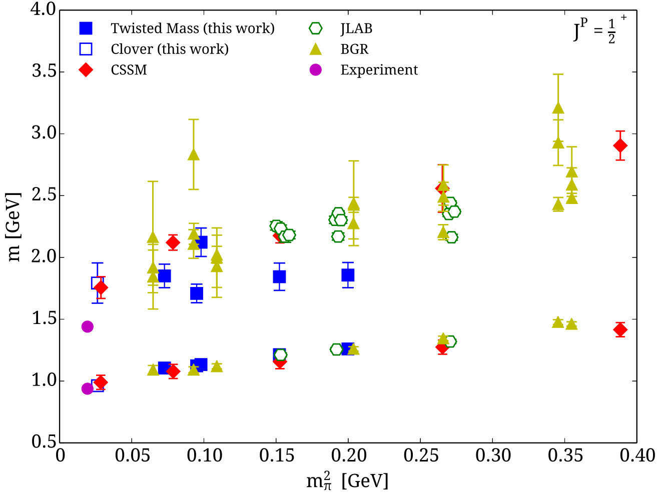

Athens Model Independent Analysis Scheme (AMIAS)

- “Novel analysis method for excited states in lattice QCD:
  The nucleon case,”
  C. Alexandrou, T. Leontiou, C. N. Papanicolas and E. Stiliaris,
  Phys. Rev. D **91** (2015) 1, 014506
  arXiv:1411.6765 [hep-lat].

Athens Model Independent Analysis Scheme (AMIAS)

- Does not rely on plateau identification of effective masses

Athens Model Independent Analysis Scheme (AMIAS)

- Does not rely on plateau identification of effective masses
- Exploits small time separations where the excited states contribute and statistical errors are small.

Athens Model Independent Analysis Scheme (AMIAS)

- Does not rely on plateau identification of effective masses
- Exploits small time separations where the excited states contribute and statistical errors are small.
- The Correlation matrix has the spectral decomposition

$$G_{ij}(t) = \sum_{\alpha=0}^{N_{\rm states}} A_i^{\alpha}\, A_j^{\dagger\alpha}\, e^{-E_\alpha\, t}\,. \quad i,j = 1,\ldots,N_{\rm interpolators}\,.$$

Athens Model Independent Analysis Scheme (AMIAS)

- Does not rely on plateau identification of effective masses
- Exploits small time separations where the excited states contribute and statistical errors are small.
- The Correlation matrix has the spectral decomposition

$$G_{ij}(t) = \sum_{\alpha=0}^{N_{\mathrm{states}}} A_i^{\alpha}\, A_j^{\dagger\alpha}\, e^{-E_\alpha\, t}\,. \quad i, j = 1, \ldots, N_{\mathrm{interpolators}}\,.$$

- Importance sampling is used to select fit parameters, A_i^{α} and E_α, with the probability $\exp(-\chi^2/2)$.

Athens Model Independent Analysis Scheme (AMIAS)

- Does not rely on plateau identification of effective masses
- Exploits small time separations where the excited states contribute and statistical errors are small.
- The Correlation matrix has the spectral decomposition

$$G_{ij}(t) = \sum_{\alpha=0}^{N_{\rm states}} A_i^{\alpha} A_j^{\dagger\alpha} e^{-E_\alpha t} . \quad i,j = 1, \ldots, N_{\rm interpolators} .$$

- Importance sampling is used to select fit parameters, A_i^{α} and E_α, with the probability $\exp(-\chi^2/2)$.
  - A parallel tempering algorithm is used to avoid local minima traps.

Athens Model Independent Analysis Scheme (AMIAS)

- Does not rely on plateau identification of effective masses
- Exploits small time separations where the excited states contribute and statistical errors are small.
- The Correlation matrix has the spectral decomposition

$$G_{ij}(t) = \sum_{\alpha=0}^{N_{\mathrm{states}}} A_i^{\alpha} A_j^{\dagger\alpha} e^{-E_\alpha t} . \quad i, j = 1, \ldots, N_{\mathrm{interpolators}} .$$

- Importance sampling is used to select fit parameters, A_i^α and E_α, with the probability $\exp(-\chi^2/2)$.
  - A parallel tempering algorithm is used to avoid local minima traps.
- Parameters are determined by fitting a Gaussian to their probability distributions.

Athens Model Independent Analysis Scheme (AMIAS)

- Does not rely on plateau identification of effective masses
- Exploits small time separations where the excited states contribute and statistical errors are small.
- The Correlation matrix has the spectral decomposition

$$G_{ij}(t) = \sum_{\alpha=0}^{N_{\rm states}} A_i^{\alpha} \, A_j^{\dagger\alpha} \, e^{-E_\alpha \, t} \, . \quad i, j = 1, \ldots, N_{\rm interpolators} \, .$$

- Importance sampling is used to select fit parameters, A_i^{α} and E_α, with the probability $\exp(-\chi^2/2)$.
  - A parallel tempering algorithm is used to avoid local minima traps.
- Parameters are determined by fitting a Gaussian to their probability distributions.
- Increase $N_{\rm states}$ until there is no sensitivity to additional exponentials.

Determining $N_{\mathrm{states}} \equiv \mathrm{n}_{\max}$ (Cyprus)

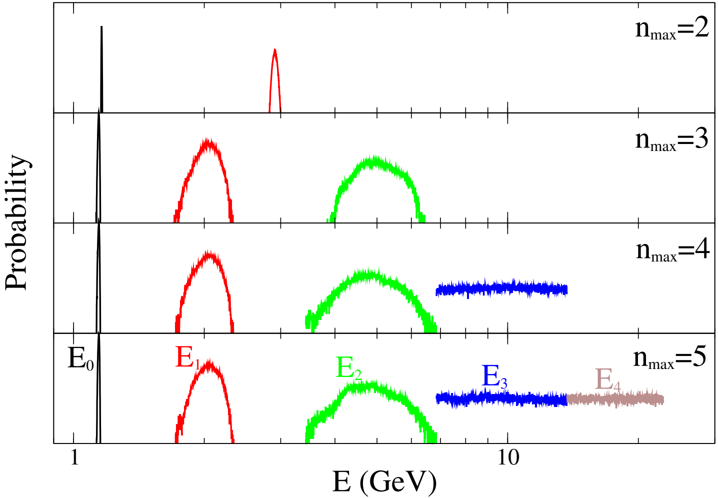

Analysis of Correlation Matrix is Essential

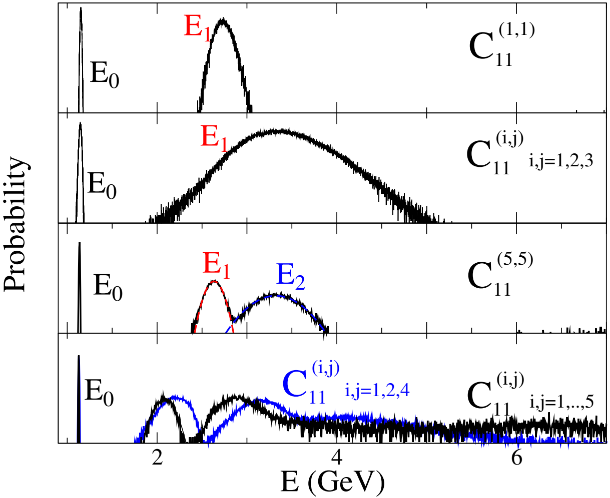

Dispersion Relation Test for the $\Lambda(1405)$

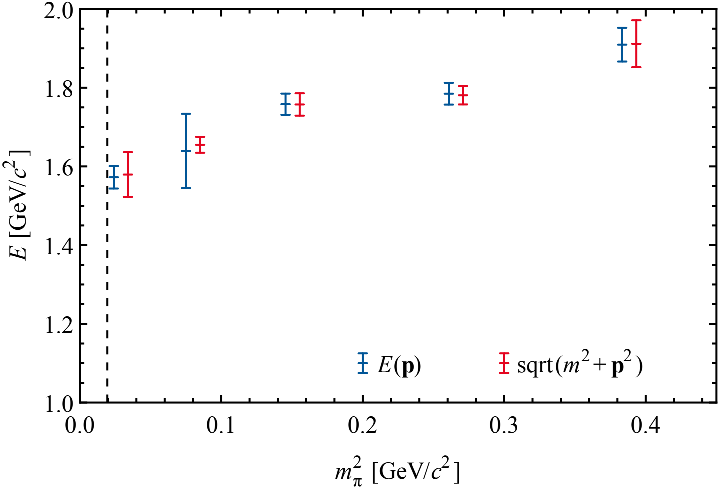

$\mathcal{G}_\mathrm{E}$ for the $\Lambda(1405)$

When compared to the ground state, the results for $\mathcal{G}_\mathrm{E}$ are consistent with the development of a non-trivial $\overline{\mathrm{K}}\mathrm{N}$ component at light quark masses.

$\mathcal{G}_{\mathrm{E}}$ for the $\Lambda(1405)$

When compared to the ground state, the results for $\mathcal{G}_{\mathrm{E}}$ are consistent with the development of a non-trivial $\overline{\mathrm{K}}\mathrm{N}$ component at light quark masses.

- Noting that the centre of mass of the $\overline{K}(s, \overline{\ell})\ N(\ell, u, d)$ is nearer the heavier N,
    - The anti–light-quark contribution, $\overline{\ell}$, is distributed further out by the $\overline{\mathrm{K}}$ and leaves an enhanced light-quark form factor.

$\mathcal{G}_E$ for the $\Lambda(1405)$

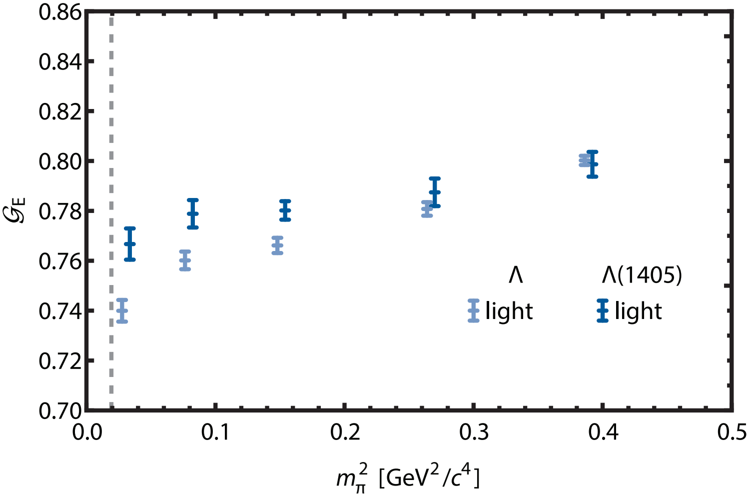

$\mathcal{G}_{\mathrm{E}}$ for the $\Lambda(1405)$

When compared to the ground state, the results for $\mathcal{G}_{\mathrm{E}}$ are consistent with the development of a non-trivial $\overline{\mathrm{K}}\mathrm{N}$ component at light quark masses.

- Noting that the centre of mass of the $\overline{K}(s,\bar{\ell})\ N(\ell,u,d)$ is nearer the heavier N,
  - The anti–light-quark contribution, $\bar{\ell}$, is distributed further out by the $\overline{\mathrm{K}}$ and leaves an enhanced light-quark form factor.
  - The strange quark may be distributed further out by the $\overline{\mathrm{K}}$ and thus have a smaller form factor.

$\mathcal{G}_E$ for the $\Lambda(1405)$

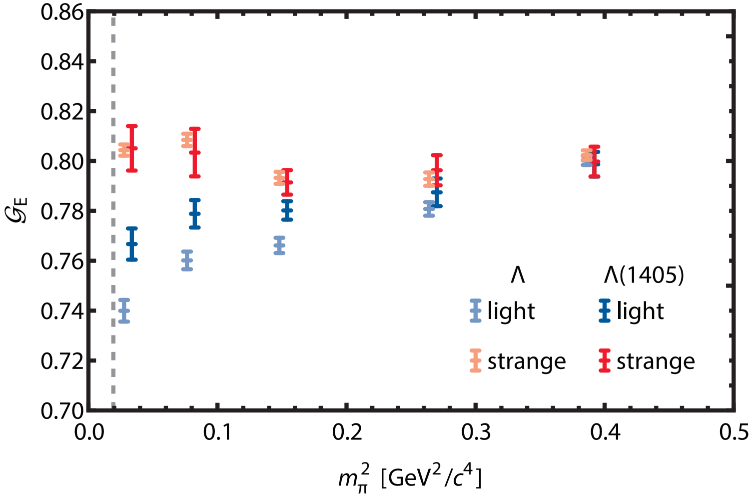

Excited State Form Factors

- The eigenstate-projected three-point correlation function is

$$\begin{aligned} G^{\mu}_{\alpha}(\mathbf{p}', \mathbf{p}; t_2, t_1) &= \sum_{\mathbf{x}_1, \mathbf{x}_2} \mathrm{e}^{-\mathrm{i}\,\mathbf{p}' \cdot \mathbf{x}_2} \mathrm{e}^{\mathrm{i}(\mathbf{p}' - \mathbf{p}) \cdot \mathbf{x}_1} \times \\ &\qquad \times \langle \Omega | v^{\alpha}_{i}(\mathbf{p}')\, \chi_i(x_2)\, j^{\mu}(x_1)\, \overline{\chi}_j(0)\, u^{\alpha}_{i}(\mathbf{p}) | \Omega \rangle \\ &= \mathbf{v}^{\alpha\,\mathsf{T}}(\mathbf{p}')\, G^{\mu}_{ij}(\mathbf{p}', \mathbf{p}; t_2, t_1)\, \mathbf{u}^{\alpha}(\mathbf{p}) \end{aligned}$$

where

$$G^{\mu}_{ij}(\mathbf{p}', \mathbf{p}; t_2, t_1) = \sum_{\mathbf{x}_1, \mathbf{x}_2} \mathrm{e}^{-\mathrm{i}\,\mathbf{p}' \cdot \mathbf{x}_2} \mathrm{e}^{\mathrm{i}(\mathbf{p}' - \mathbf{p}) \cdot \mathbf{x}_1} \langle \Omega | \chi_i(x_2)\, j^{\mu}(x_1)\, \overline{\chi}_j(0) | \Omega \rangle$$

is the matrix constructed from the three-point correlation functions of the original operators $\{ \chi_i \}$.

Extracting Form Factors from Lattice QCD

- To eliminate the time dependence of the three-point correlation function, we construct the ratio

$$R^{\mu}_{\alpha}(\mathbf{p}', \mathbf{p}; t_2, t_1) = \left(\frac{G^{\mu}_{\alpha}(\mathbf{p}', \mathbf{p}; t_2, t_1)\, G^{\mu}_{\alpha}(\mathbf{p}, \mathbf{p}'; t_2, t_1)}{G_{\alpha}(\mathbf{p}'; t_2)\, G_{\alpha}(\mathbf{p}; t_2)} \right)^{1/2}$$

Extracting Form Factors from Lattice QCD

- To eliminate the time dependence of the three-point correlation function, we construct the ratio

$$R^{\mu}_{\alpha}(\mathbf{p}', \mathbf{p}; t_2, t_1) = \left(\frac{G^{\mu}_{\alpha}(\mathbf{p}', \mathbf{p}; t_2, t_1)\, G^{\mu}_{\alpha}(\mathbf{p}, \mathbf{p}'; t_2, t_1)}{G_{\alpha}(\mathbf{p}'; t_2)\, G_{\alpha}(\mathbf{p}; t_2)} \right)^{1/2}$$

- To further simply things, we define the reduced ratio

$$\overline{R}^{\mu}_{\alpha} = \left(\frac{2E_{\alpha}(\mathbf{p})}{E_{\alpha}(\mathbf{p}) + m_{\alpha}} \right)^{1/2} \left(\frac{2E_{\alpha}(\mathbf{p}')}{E_{\alpha}(\mathbf{p}') + m_{\alpha}} \right)^{1/2} R^{\mu}_{\alpha}$$

Current Matrix Element for Spin-1/2 Baryons

The current matrix element for spin-1/2 baryons has the form

$$\langle p', s' | j^\mu | p, s \rangle = \left(\frac{m_\alpha^2}{E_\alpha(\mathbf{p}) E_\alpha(\mathbf{p}')} \right)^{1/2} \times$$
$$\times\, \overline{u}(\mathbf{p}') \left(F_1(q^2)\, \gamma^\mu + \mathrm{i}\, F_2(q^2)\, \sigma^{\mu\nu} \frac{q^\nu}{2 m_\alpha} \right) u(\mathbf{p})$$

Current Matrix Element for Spin-1/2 Baryons

The current matrix element for spin-1/2 baryons has the form

$$\langle p', s' | j^\mu | p, s \rangle = \left(\frac{m_\alpha^2}{E_\alpha(\mathbf{p}) E_\alpha(\mathbf{p}')} \right)^{1/2} \times$$
$$\times\, \overline{u}(\mathbf{p}') \left(F_1(q^2)\, \gamma^\mu + \mathrm{i}\, F_2(q^2)\, \sigma^{\mu\nu} \frac{q^\nu}{2m_\alpha} \right) u(\mathbf{p})$$

- The Dirac and Pauli form factors are related to the Sachs form factors through

$$\mathcal{G}_\mathrm{E}(q^2) = F_1(q^2) - \frac{q^2}{(2m^\alpha)^2} F_2(q^2)$$
$$\mathcal{G}_\mathrm{M}(q^2) = F_1(q^2) + F_2(q^2)$$

Sachs Form Factors for Spin-1/2 Baryons

- A suitable choice of momentum ($\mathbf{q} = (q, 0, 0)$) and the (implicit) Dirac matrices allows us to directly access the Sachs form factors:
  - for $\mathcal{G}_{\mathrm{E}}$: using $\Gamma_4^{\pm}$ for both two- and three-point,

$$\mathcal{G}_{\mathrm{E}}^{\alpha}(q^2) = \overline{R}_{\alpha}^{4}(\mathbf{q}, \mathbf{0}; t_2, t_1)$$

  - for $\mathcal{G}_{\mathrm{M}}$: using $\Gamma_4^{\pm}$ for two-point and $\Gamma_j^{\pm}$ for three-point,

$$|\varepsilon_{ijk}\, q^i|\, \mathcal{G}_{\mathrm{M}}^{\alpha}(q^2) = (E_{\alpha}(\mathbf{q}) + m_{\alpha})\, \overline{R}_{\alpha}^{k}(\mathbf{q}, \mathbf{0}; t_2, t_1)$$

  - where for positive parity states,

$$\Gamma_j^{+} = \frac{1}{2}\begin{bmatrix} \sigma_j & 0 \\ 0 & 0 \end{bmatrix} \qquad \Gamma_4^{+} = \frac{1}{2}\begin{bmatrix} \mathbb{I} & 0 \\ 0 & 0 \end{bmatrix}$$

    and for negative parity states,

$$\Gamma_j^{-} = -\gamma_5 \Gamma_j^{+} \gamma_5 = -\frac{1}{2}\begin{bmatrix} 0 & 0 \\ 0 & \sigma_j \end{bmatrix} \qquad \Gamma_4^{-} = -\gamma_5 \Gamma_4^{+} \gamma_5 = -\frac{1}{2}\begin{bmatrix} 0 & 0 \\ 0 & \mathbb{I} \end{bmatrix}$$

Finite Volume Dependence of the Λ Spectrum